DISSERTATIONES SCHOLAE DOCTORALIS AD SANITATEM INVESTIGANDAM
UNIVERSITATIS HELSINKIENSIS

FELIX SIEBENHÜHNER

THE ROLE OF MULTI-SCALE PHASE SYNCHRONIZATION AND CROSS-FREQUENCY INTERACTIONS IN COGNITIVE INTEGRATION

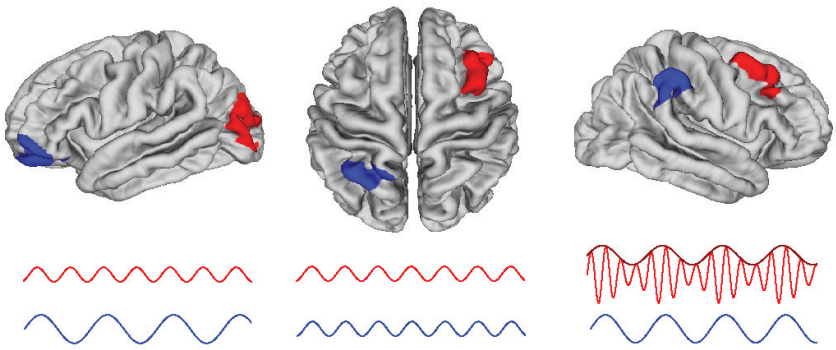

HELSINKI INSTITUTE OF LIFE SCIENCE (HiLIFE)
NEUROSCIENCE CENTER
DIVISION OF PHYSIOLOGY AND NEUROSCIENCE
DEPARTMENT OF BIOSCIENCES
FACULTY OF BIOLOGICAL AND ENVIRONMENTAL SCIENCES
DOCTORAL PROGRAMME BRAIN & MIND
UNIVERSITY OF HELSINKI

The role of multi-scale phase synchronization and cross-frequency interactions in cognitive integration

Felix Siebenhühner

Helsinki Institute of Life Science
Neuroscience Center
Division of Physiology and Neuroscience
Faculty of Biological and Environmental Sciences
Doctoral Programme Brain and Mind
University of Helsinki

ACADEMIC DISSERTATION

To be presented for public examination with the permission of the Faculty of Biological and Environmental Sciences of the University of Helsinki

in Haartman Institute, Hall 1, 21.05.2019

Helsinki, 2019

Supervisors	Docent Satu Palva, PhD Helsinki Institute of Life Science, Neuroscience Center, Helsinki University, Finland Docent J. Matias Palva, PhD Helsinki Institute of Life Science, Neuroscience Center, Helsinki University, Finland
Pre-examiners	Professor Paul Sauseng, PhD Department of Psychology, Ludwig-Maximilian-Universität München, Germany Professor Niko Busch, PhD Department of Psychology, Westfälische Wilhelms-Universität Münster, Germany
Thesis Advisory Committee	Docent Henri Huttunen, PhD Neuroscience Center, Helsinki Institute of Life Science, Helsinki University, Finland Teemu Rinne, PhD Turku Brain and Mind Center, University of Turku, Finland
Opponent	Associate Professor Michael X Cohen, PhD Donders Centre for Neuroscience, Radboud University, Nijmegen, Netherlands
Custos	Professor Juha Voipio, PhD Molecular and Integrative Biosciences Research Programme, Helsinki University, Finland

ISBN 978-951-51-5219-0 (print) and ISBN 978-951-51-5220-6 (online)
ISSN 2342-3161 (print) and ISSN 2342-317X (online)

Only a palace, with interior doors,
Well painted, well gargoyled, with multiple floors.
Two windows let free this projector machine,
And a magical world here appears on the screen.
My servants attend me with tricks of the senses,
The past and the future and similar tenses.
And on platters of air they convey me my measure,
Both gladness and sorrow, I lack not for treasure.
The lord and his lady are seated within
In the court of the mind where the song does begin.
The song is as fine, is as fine, is as follows…

"The Head", by Robin Williamson, 1968

Table of Contents

Original publications

This thesis is based on the following publications:

I. M. Lobier, **F. Siebenhühner**, S. Palva, J. M. Palva: Phase transfer entropy: A novel phase-based measure for directed connectivity in networks coupled by oscillatory interactions*, NeuroImage* 85:853-872, 2014

II. **F. Siebenhühner**, S. H. Wang, J. M. Palva, S. Palva: Cross-frequency synchronization connects networks of fast and slow oscillations during visual working memory maintenance, *eLife*: e13451, 2016

III. S. Rouhinen, **F. Siebenhühner**, J. M. Palva, S. Palva: Spectral and anatomical patterns of large-scale synchronization predict human attentional capacity, *under preparation for re-submission to Cerebral Cortex*

IV. **F. Siebenhühner**, S. H. Wang, G. Arnulfo, L. Nobili, J. M. Palva, S. Palva: Resting-state cross-frequency coupling networks in human electrophysiological recordings*, under revision for PLoS Biology*

All studies designed and conducted under the active supervision of Satu Palva and J. Matias Palva. Author's contribution to the publications included in the thesis:

I. The candidate together with ML developed software and performed simulations and analyzed simulated data. All authors wrote the manuscript together.

II. SP and JMP designed the experiment and SP collected M/EEG data. The candidate performed data pre-processing, carried out data analysis, and together with SHW and JMP developed software for the analysis of cross-frequency interactions. The candidate wrote the manuscript together with JMP and SP.

III. SR collected M/EEG data and analyzed local oscillations and networks of 1:1 phase synchronization. The candidate performed analysis of cross-frequency interactions and wrote the corresponding parts of the manuscript. The non-CF parts of the manuscript were written by SR, JMP and SP.

IV. The candidate recorded and preprocessed MEG data. SEEG data were collected by GA and LN and preprocessed by GA and SHW. The candidate developed the data-analysis software together with SHW and GA, carried out data analysis, and wrote the manuscript together with JMP and SP.

Publication **III** was also used in the dissertation of Santeri Rouhinen.

List of general abbreviations

BOLD	Blood Oxygen Level Dependent
CF	Cross-Frequency
CFC	Cross-Frequency Coupling
CFS	Cross-Frequency Phase Synchrony
cPLV	complex Phase Locking Value
AAC	Amplitude-Amplitude Coupling
EEG	Electroencephalography
fMRI	functional Magnetic Resonance Imaging
iEEG	intracranial Electroencephalography
iPLV	imaginary Phase Locking Value
HF	High-Frequency
HR	Hit Rate
LF	Low-Frequency
LFP	Local Field Potential
MEG	Magnetoencephalography
M/EEG	Magneto- and electroencephalography
MI	Mutual Information
MRI	Magnetic Resonance Imaging
PAC	Phase-Amplitude Coupling
PFC	Prefrontal cortex
PPC	Posterior Parietal Cortex
PLV	Phase Locking Value
PS	Phase Synchrony
SEEG	Stereo-Electroencephalography
SNR	Signal-to-Noise-Ratio
TE	Transfer Entropy
VC	Volume Conduction
VWM	Visual Working Memory
WM	Working Memory
wPLI	weighted Phase-Lag Index

Abstract

Neuronal processing is distributed into anatomically distinct, largely specialized, neuronal populations. These populations undergo rhythmic fluctuations in excitability, which are commonly known as neuronal oscillations. Electrophysiological studies of neuronal activity have shown that phase synchronization of oscillations within frequencies characterizes both resting state and task execution and that its strength is correlated with task performance. Therefore phase-synchronization within frequencies is thought to support communication between oscillating neuronal populations and thereby integration and coordination of anatomically distributed processing in cognitive functions. However, it has remained open if and how phase synchronization is associated with directional flow of information. Furthermore, oscillations and synchronization are observed concurrently in multiple frequencies, which are thought to underlie distinct computational functions. Little is known how oscillations and synchronized networks of different frequencies in the human brain are integrated and enable unified cognitive function and experience.

In the first study of this thesis, we developed a measure of directed connectivity in networks of coupled oscillators, called Phase Transfer Entropy (Phase TE) and tested if Phase TE could detect directional flow in simulated data in the presence of noise and signal mixing. Results showed that Phase TE indeed reliably detected information flow under these conditions and was computationally efficient.

In the other three studies, we investigated if two different forms of inter-areal cross-frequency coupling (CFC), namely cross-frequency phase synchrony (CFS) and phase-amplitude coupling (PAC), could support integration and coordination of neuronal processing distributed across frequency bands in the human brain.

In the second study, we analyzed source-reconstructed magneto- and electroencephalographic (M/EEG) data to investigate whether inter-areal CFS could be observed between within-frequency synchronized networks and thereby support the coordination of spectrally distributed processing in visual working memory (VWM). The results showed that CFS was increased during VWM maintenance among theta to gamma frequency bands and the strength of CFS networks predicted individual VWM capacity. Spectral patterns of CFS were found to be different from PAC, indicating complementary roles for both mechanisms.

In the third study, we analyzed source-reconstructed M/EEG data to investigate whether inter-areal CFS and PAC could be observed during two multi-object visual tracking tasks and thereby support visual attention. PAC was found to be significantly correlated with object load in both tasks, and CFS in one task. Further, patterns of CFS and PAC differed significantly between subjects with high and low capacity for visual attention.

In the fourth study, we analyzed intracerebral stereo-electroencephalographic data (SEEG) and source-reconstructed MEG data to investigate whether CFS and PAC are present also in resting state. Further, in order to address concerns about observations of CFC being spurious and caused by non-sinusoidal or non-zero mean signal waveforms, we introduced a new approach to identify true inter-areal CFC connections and discard potentially spurious ones. We observed both inter-areal CFS and PAC, and showed that a significant part of connections was unambiguously true and non-spurious. Spatial profiles differed between CFS and PAC, but were consistent across datasets.

Together, the results from studies II-IV provide evidence that inter-areal CFS and PAC, in complementary ways, connect frequency-specific phase-synchronized networks that involve functionally specialized regions across the cortex to support complex functions such as VWM and attention, and also characterize the resting state. Inter-areal CFC thus may be crucial for the coordination and integration of spectrally distributed processing and the emergence of introspectively coherent cognitive function.

Tiivistelmä

Keskeinen kysymys aivotutkimuksessa on, kuinka ajattelu ja kognitio syntyvät ihmisaivojen 10^15 hermosolussa. Informaation käsittely aivoissa tapahtuu suurissa hermosolupopulaatioissa, jotka ovat toiminnallisesti erikoistuneita ja anatomisesti eroteltuja eri aivoalueille. Niiden aktivaatiorakenteiden jaksollisia muutoksia kutsutaan aivorytmeiksi eli oskillaatioiksi. Hermosolupopulaatioiden välistä viestintää edesauttaa niiden toiminnan samantahtisuus eli synkronoituminen. Sähköfysiologisissa tutkimuksissa on havaittu aivorytmien synkronoituvan sekä lepomittausten että tehtävien suorituksen aikana siten että tämä synkronoituminen ennustaa kognitiivissa tehtävissä suoriutumista.

Oskillaatioiden vaihesynkronia ei kuitenkaan kerro niiden välisen vuorovaikutuksen suunnasta. Tämän lisäksi oskillaatioita ja niiden välistä synkroniaa havaitaan yhtäaikaisesti lukuisilla eri taajuuksilla, joiden ajatellaan olevan vastuussa erillisistä laskennallisista ja kognitiivisista toiminnoista. Toistaiseksi on kuitenkin jäänyt kartoittamatta, miten informaation käsittely eri taajuuksilla yhdistetään yhtenäisiksi kognitiivisiksi toiminnoiksi, ja havaitaanko myös eri taajuisten oskillaatioverkkojen välillä synkroniaa.

Väitöskirjan ensimmäisessä osatyössä on kehitetty uusi tapata mitata oskillaattoriverkkojen vuorovaikutusten suuntia, jonka toimivuus todennettiin simuloimalla synkronoituneita hermosolupopulaatioita.

Väitöskirjan muissa osatöissä on tutkittu havaitaanko ihmisaivoissa eri taajuisten oskillaatioiden välistä synkronoitumista. Erityisesti tutkittiin kahta erilaista synkronian muotoa, joista ensimmäinen (’cross- frequency phase synchrony’,CFS) mittaa kahden oskillaation välistä vaihesuhdetta ja toinen (’phase-amplitude coupling’, PAC) vaiheen ja amplitudin suhdetta.

Väitöskirjan toisessa osassa tutkittiin, selittääkö CFS koehenkilöiden suoriutumista näkötyömuistitehtävässä. Tutkimukseen osallistuneilta koehenkilöiltä mitattiin aivosähkökäyrä (EEG) ja aivomagneettikäyrä (MEG), joiden avulla selvitettiin havaitaanko aivoalueiden välistä synkroniaa (CFS). Tutkimustulokset osoittivat, että koehenkilöiden CFS oli korkeampi näkötyömuistitehtävän mielessä pitämisen aikana theta-taajuuksista gamma-taajuuksiin asti ja että CFS-verkkojen vahvuus ennusti yksilöllistä työmuistikapasiteettia. Kolmannessa tutkimuksessa analysoitiin MEG- ja EEG-aivokuvantamislaitteita käyttäen onko aivoalueiden välillä CFS:ä ja PAC:a kahdessa näkötarkkaavaisuustehtävässä. PAC lisääntyi tilastollisesti merkitsevästi tehtävän vaikeuden mukaan kummassakin tehtävässä, kun taas CFS lisääntyi yhdessä tehtävässä. Lisäksi CFS ja PAC taajuusparit olivat erilaisia hyvin suoriutuvien koehenkilöiden sekä heikosti suoriutuvien koehenkilöiden välillä.

Neljännessä tutkimuksessa tutkittiin havaitaanko CFS:ä ja PAC:a aivojen lepotilassa. Aivokuoren aktiivisuutta mitattiin MEG:llä sekä epilepsiapotilailta aivoihin kirurgisesti asetetuilla elektrodeilla. CFS:ä sekä PAC:a havaittiin kummallakin menetelmällä. Lisäksi kehitimme menetelmän joka vähentää väärien havaintojen todennäköisyyttä ja lisää aitojen CFS ja PAC yhteyksien havaitsemista. Tulokset osoittavat, että merkittävä osuus yhteyksistä aivoalueiden välillä on aitoja. CFS- ja PAC-profiilit erosivat toisistaan, mutta olivat samanlaisia eri menetelmillä tutkittaessa.

Yhdistettynä tulokset tutkimuksista II–IV viittaavat siihen, että CFS ja PAC yhdistävät eri taajuuksille ja aivoalueille hajautettua informaation käsittelyä. CFS:sää ja PAC:ia havaittiin aivojen lepotilassa mutta myös tarkkaavaisuus- ja näkötyömuistitehtävän aikana. CFS ja PAC saattavat mahdollistaa eri taajuisten aivorytmien ja hajautettujen prosessien koordinaation ja yhdistämisen.

1. Background

How does cognition arise from the activity of hundreds of billions of neurons? This question has occupied and puzzled researchers and interested laypeople ever since the existence of the neuron as the fundamental unit of the brain was proven in the 19th century by Santiago Ramón y Cajal (López-Muñoz et al., 2006). Neurons are known to communicate via electrical and chemical signaling, however cognitive function can only be understood by studying their collective behaviour in neuronal populations and the interactions between these populations. Advances in neuroimaging techniques, which allow to record the electrical activity of populations of neurons with high temporal and spatial precision, together with advanced computational hard- and software for the analysis of such signals, have allowed researchers in the last decades to elucidate basic principles of large-scale communication between neuronal populations. In particular, the study of oscillatory activity of neuronal populations and synchronization between these has provided evidence that task-specific phase-synchronized networks in different frequency bands support cognitive functions. However, many questions have remained unanswered, such as how information transfer can be measured in networks of oscillations, and how distinct phase-synchronized networks at different frequencies in the human brain are integrated to enable unified cognitive functioning and experience.

1.1 The organization of the human cortex

The human brain is comprised of the cerebral cortex, the cerebellum and subcortical structures. The cerebral cortex is the seat of higher cognitive functions such as attention, conscious awareness, working memory, language, problem solving, and deliberate decision-making, while the cerebellum is thought to primarily support motor function, and subcortical structures are associated with a variety of functions such as relaying sensory information, maintaining homeostasis, consciousness regulation, emotional reactions, motor control and memory. The cerebral cortex is layered and has two main components the allocortex, and the neocortex. The allocortex, comprising of the hippocampus and the olfactory cortex consists of 3 to 4 layers, whereas the neocortex consists of 6 layers, of which I is the most superficial and VI the deepest. The different types of neurons found in the cerebral cortex are distributed differentially across cortical layers. The cortex is folded, and the main gyri and sulci (ridges and grooves) are used as anatomical landmarks in parcellations of the brain. The most basic division of the cortex is that into the four lobes, namely the frontal, occipital, parietal and temporal lobes. Individual regions of the cortex are functionally specialized and complex functions such as attention, working memory,

language, arithmetics and decision-making arise from the interplay of several regions in functional networks. Communication between neurons takes place at synapses, which connect a terminal on the presynaptic axon and a target on the postsynaptic neuron. There are two major types of synapses: Electric synapses, where an electric current is transmitted across a gap junction channel, and which are only involved in short-range communication. In contrast, axons for chemical signaling span the whole cortex and allow signaling between distant neurons at chemical synapses, where chemical transmitters are released from the presynaptic cells, diffused across the synaptic cleft and bind to receptors on the surface of the postsynaptic cell. Within neurons, signals travel along the axon in form of an action potential, and a neuron emitting an action potential is also said to “fire” or “spike”.

1.2 Working memory and attentional functions

Two important cognitive higher-order functions realized in the cerebral cortex are working memory and attention. Working memory (WM) denotes the storage of information for immediate access and utilization over a short time of up to a few seconds. The short-term maintenance of visual information and visual object representations is called visual working memory (VWM). VWM may be studied using e.g. delayed match-to-sample tasks, in which a multi-object stimulus must be kept in memory and then compared to a second version of the stimulus, where some objects may have been altered. Its capacity, i.e. the number of objects that can be stored reliably in VWM, varies between individuals, but in delayed match-to-sample VWM tasks the capacity is typically between 3 and 4 (Luck and Vogel, 1997).

The neuronal mechanism of VWM has been investigated in a number of studies using functional magnetic resonance imaging (fMRI). These studies have shown that VWM involves concurrent neuronal activity of many brain regions. While the maintenance of perceived objects is generally localized to the visual cortex (Emrich et al., 2013; Kravitz et al., 2013; Riggall and Postle, 2012), central executive control, i.e. regulation, manipulation and utilization of objects stored in VWM for subsequent action, has been shown to be localized to the frontal cortex, particularly to the lateral prefrontal cortex (lPFC) (Markowitz et al., 2015; Rowe et al., 2000; Sreenivasan et al., 2014). Memory retrieval, in contrast, has been associated with the posterior parietal cortex (Jones and Berryhill, 2012; Munk et al., 2002).

Visual attention denotes the maintained focus on one or more selected objects in the visual representation of the environment. Similarly to VWM, the capacity of objects that can effectively be attended simultaneously is 2-4 (Pylyshyn and Storm, 1988; Treisman, 2006). Also similarly to VWM, fMRI studies have shown that activity in the visual, prefrontal and posterior parietal regions has been correlated with performance in visual attention tasks

(Alnaes et al., 2015; Culham et al., 1998; Howe et al., 2009; Jovicich et al., 2001). In addition to the two functions being based on similar cortical regions, the individual capacities of VWM and visual attention have also been found to be correlated (Oksama and Hyona, 2004).

1.3 Network interactions in the brain

Since higher-order cognitive functions are enabled by regions that are not directly adjacent, but distributed over the cortex, it has been proposed that the brain is organized into functional networks consisting of different regions which are connected by long-range axons tracts, and signaling along these tracts enables communication between these regions, allowing for the emergence of complex cognitive functions. In resting-state studies with functional magnetic resonance imaging (fMRI) several networks were identified whose regions showed correlations of blood oxygen level dependent (BOLD) signal fluctuations (Fox et al., 2005; Raichle et al., 2001). Some of these resting-state networks (RSNs) were found to exhibit high similarity to stipulated networks for particular cognitive functions or sensory processing. For example, there were identified two distinct, but interacting, networks supporting attention in the human cortex, a dorsal network for top-down modulation including the intraparietal cortex and superior frontal cortex; and a ventral salience network for detection of salient or unexpected relevant stimuli including the temporoparietal cortex and inferior frontal cortex (Corbetta and Shulman, 2002; Corbetta et al., 2008; Fox et al., 2006). Other networks include the frontoparietal control network, visual, auditory and sensorimotor networks, as well as the so-called default mode network which is particularly active during the resting state itself, but attenuated during task execution (Raichle et al., 2001; Raichle, 2015).

1.4 Neuronal oscillations as a mechanism of cortical computations

Neuronal processing is distributed into anatomically distant neuronal populations that largely fulfill specialized functional roles. Such populations exhibit neuronal oscillations, i.e. collective rhythmic fluctuations in excitability and firing patterns. Such coordinated activity within populations has also been described as local synchronization (Engel et al., 2001; Singer, 1999), which must not be confused with large-scale synchrony between populations (see 1.6). Hence, oscillations impose excitability windows that regulate neuronal activity in local networks. In such population oscillations, the individual neurons' firing patterns can be but need not be periodical, but crucially the collective firing patterns are described stochastically by a sine function. Oscillatory activity in a group of neurons can be entrained by an external input, e.g. gamma oscillations induced by visual stimuli (Gray et al., 1989), but can also arise intrinsically through various mechanisms involving locally interconnected

groups of excitatory neurons, of inhibitory neurons or both (Fries, 2015; Wang, 2010). Unlike individual spikes, which can only be seen in single-cell recordings, postsynaptic currents from many spiking neurons whose collective firing is ruled by oscillations can be detected with large-scale electrophysiological neuroimaging methods such as MEG and EEG (see 1.8 and 3.1.2).

Oscillations can be characterized by their amplitude, phase and frequency. While the frequency of an oscillation denotes the inverse of a length of a cycle, the phase indicates the current position on the sine wave and the amplitude its maximal absolute value. In neuronal oscillations, the overall excitability of a population is highest at the peak and lowest at the through and a larger amplitude reflects larger local synchronization.

1.5 The functional significance of oscillations in cognitive functions

Neuronal oscillations are grouped into frequency bands. This grouping is historical and the range of individual bands can vary in the literature. In this thesis, the following ranges are used: Delta (δ): 1-4 Hz, theta (θ): 4-8 Hz, alpha (α): 8-15 Hz, beta (β): 15-30 Hz, gamma (γ): 30-120 Hz. Importantly, oscillatory activity can also be present at frequencies that do not show a clear peak in the amplitude spectrum in electrophysiological neuroimaging.

Alpha (α) oscillations, which are clearly visible in EEG recordings and strongest in occipital and parietal cortices (Groppe et al., 2013), are particularly prominent during drowsy and inattentive states, but also during some highly demanding tasks. One prominent hypothesis about α oscillations is that their primary function is inhibition of task-unrelated regions (Jensen and Mazaheri, 2010; Klimesch et al., 2007). Indeed, task performance is correlated with suppression of α amplitudes in early sensory regions that process task-irrelevant information (Händel et al., 2011; Sauseng et al., 2009) or motor regions (Hummel et al., 2002). However, α oscillations have also been found to exhibit positive correlations with task-related neuronal processing in higher-level sensory as well as attentional and executive regions (Jensen et al., 2015; Klimesch, 2012; Palva and Palva, 2007; Palva and Palva, 2011; Sauseng et al., 2005; Sauseng et al., 2005; Schroeder et al., 2018). Additionally, there is evidence that α oscillations provide the rhythm for sampling of visual information (Busch and VanRullen, 2010; Drewes and Vanrullen, 2011; Dugue et al., 2011; Hanslmayr et al., 2013; Mathewson et al., 2009).

Below the α band, theta (θ) oscillations have been studied extensively in rodent hippocampus, where they span the range 4-12 Hz and are associated with navigation, and memory formation (O'Keefe and Recce, 1993; Vanderwolf, 1969; Vertes, 1977; Winson, 1974). In humans, θ oscillations span the range 4–8 Hz. Similarly to rodents, hippocampal

theta in humans has been shown to support navigation and memory formation (Bohbot et al., 2016; Bush et al., 2017; Lega et al., 2012). However, θ oscillations in the human cortex are considered a different phenomenon than those in the hippocampus. θ oscillations of the frontal cortex have been implicated as essential for cognitive control and decision-making (Cavanagh and Frank, 2014; Cohen and Donner, 2013) and underlying the perceptive rhythm in two-object attention (Fiebelkorn et al., 2013; Herrmann et al., 2016; Landau and Fries, 2012; Landau et al., 2015). Also, θ oscillations may underlie memory formation (Axmacher et al., 2006).

Delta (θ) oscillations have been associated with stimulus selection and entrainment to rhythmically appearing stimuli in primates (Lakatos et al., 2008) and humans (Besle et al., 2011). δ oscillations and even slower rhythms (<1 Hz) also are observed during slow-wave sleep, where they may support memory consolidation (Maquet, 2001).

Beta (β) oscillations have been associated both with sensorimotor and cognitive function, and have been suggested to underlie maintenance of the current sensorimotor or cognitive state (Engel and Fries, 2010). Further, β oscillations have been shown to support time evaluation (Kulashekhar et al., 2016) and, in a primate study, the evaluation of task-relevant information (Haegens et al., 2017).

Gamma (γ) oscillations have been linked to representation and maintenance of sensory information of perceived (Busch et al., 2006; Honkanen et al., 2015; Michalareas et al., 2016) and attended stimuli (Rouhinen et al., 2013; Vidal et al., 2006) in attention and working memory as well as multimodal integration, consciousness and motor-planning (Fries, 2015; Herrmann et al., 2004; Jensen et al., 2007; Tallon-Baudry and Bertrand, 1999; Uhlhaas et al., 2009). It has been proposed that the γ cycle acts as a fundamental computational mechanism for fast adaptive processing (Fries et al., 2007). Proposed mechanisms for the generation of γ oscillations involve local circuits of either inhibitory interneurons alone or of interneurons and excitatory pyramidal neurons, and different mechanisms might underlie the slower and faster γ oscillations (Murty et al., 2018).

1.6 Phase synchrony of oscillating neuronal assemblies

Oscillations are directly associated with rhythmic membrane potential fluctuations (Schroeder et al., 2008) so that neuronal excitability and neuronal firing follow the oscillatory phase, and is highest around the peak and lowest around the through of the oscillation cycle. This means that inputs that arrive in a population at a phase of high excitability are more likely to evoke downstream action potentials. Also, inputs that arrive simultaneously have better chances of evoking action potentials in a downstream target

neuron than asynchronous inputs because post-synaptic potentials are integrated non-linearly (Azouz and Gray, 2003; Konig et al., 1996; Singer, 1999; Singer, 2009). Thus, synchronization of excitability and firing patterns enhances signaling between neuronal populations. Based on this, the 'communication through coherence' hypothesis states that phase synchronization (PS), i.e. a sustained constant phase relationship between populations, enables constant spike time relationships and therefore effective communication and information transfer between them. (Fries, 2005; Fries, 2015).

Large-scale networks of PS at different frequencies are considered crucial for cognitive functions (Palva and Palva, 2012; Petersen and Sporns, 2015; Singer, 1999; Singer, 2009) and have been proposed to serve both for "bottom-up" and "top-down" processing of information in the brain, that are, respectively: the "feedforward" integration of sensory data and its influence on top-level cognition and decision-making; and the "feedback" control and gating of lower sensorimotor circuits by executive function and decisions (Jensen et al., 2015; Michalareas et al., 2016).

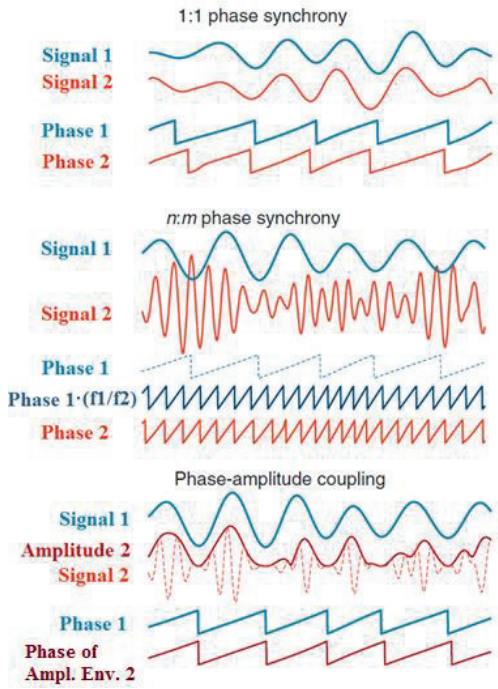

Figure 1: Phase synchrony, n:m cross-frequency phase synchrony and phase-amplitude coupling. Adapted from Palva 2012.

In particular, stimulus-driven synchronization in γ frequencies has been proposed to serve the maintenance of sensory object representation and feature binding (Engel and Singer, 2001; Singer, 1999) as well as the bottom-up processing of sensory information, while δ, θ, α or β synchronization are assumed to underlie top-down cognitive control (Bastos et al., 2015; Buschman and Miller, 2007; Jensen et al., 2015; Palva and Palva, 2007; Voloh et al., 2015). In line with this view, γ band synchrony has been found to be stronger in the more forward-projecting superficial cortical layers, whereas α and β synchrony on the other hand are stronger in the deep cortical, backwards-projecting layers (Fries, 2015).

Consequently, complex functions such as working memory and attention have been shown to involve PS networks in various frequency bands. In particular, maintenance of visual information is correlated with β and γ PS in visual and parietal regions (Salazar et al., 2012; Tallon-Baudry et al., 2001; Tallon-Baudry et al., 2004), whereas fronto-parietal α networks

have been shown to underlie attentional and executive control, facilitating the processing of relevant and the suppression of irrelevant information (Freunberger et al., 2009; Glennon et al., 2016; Palva et al., 2010; Sadaghiani et al., 2012, van Driel 2014). Further, it has been proposed that θ synchrony exerts a top-down control function from the prefrontal cortex on parietal and temporal regions and facilitates task switching during WM (Griesmayr et al., 2014; Sauseng et al., 2005; Sauseng et al., 2006; Sauseng et al., 2010) and also underlies attention reorienting (Senoussi et al., 2018). Similarly, visual attention has been implicated to be facilitated by PS in α–γ bands among frontal, posterior parietal, and visual regions (Doesburg et al., 2016; Doesburg et al., 2009; Lobier et al., 2017; Siegel et al., 2008).

PS can be quantified using various metrics, the best known of which is the phase-locking-value (PLV) (Lachaux et al., 1999). Other metrics, such as the weighted Phase-Lag Index (wPLI) (Vinck et al., 2011) or the imaginary part of the complex phase-locking value (iPLV) (Palva et al., 2018) only take into account the imaginary part of the signal, which is not affected by volume conduction, and thus report fewer artificial interactions (see also 3.3.1).

1.7 Cross-frequency coupling

While phase synchronization within frequency bands can achieve spatial integration, it does not explain how interactions between phase-synchronized networks of different frequencies can be achieved and hence what are the mechanisms that underlie the interplay of top-down and bottom-up processing. These interactions have been suggested to be mediated by several putative forms of cross-frequency coupling (CFC): phase-amplitude coupling (PAC), also sometimes called “nested oscillations” (Axmacher et al., 2010; Bahramisharif et al., 2018; Canolty et al., 2006; Cohen et al., 2009a; Cohen et al., 2009b; Keitel et al., 2018; Lakatos et al., 2005; Lakatos et al., 2013; Park et al., 2015; Park et al., 2016; Roux et al., 2013; Vanhatalo et al., 2004), phase-phase coupling, which we here refer to as cross-frequency phase synchrony (CFS) (Besle et al., 2011; Chaieb et al., 2015; Palva et al., 2005; Sauseng et al., 2008; Tass et al., 1998), amplitude-amplitude coupling (AAC) and phase-frequency coupling (PFC) (Hyafil et al., 2015).

An important distinction that has often not been made clear in past discussions of CFC is that between local and inter-areal interactions. Whereas local CFC is estimated between time series at different frequencies of the same neuronal population, inter-areal CFC is measured between time-series of different populations and different frequencies.

In the past, most research has focused on PAC, where the amplitude of a faster oscillations is modulated by the phase of a slower oscillation, to such an extent that the term “cross-

frequency coupling" has sometimes been used synonymously for PAC. Of these studies, most have focused on local PAC only, and the probably most studied form of CFC is local PAC in the rodent hippocampus (Belluscio et al., 2012; Roopun et al., 2008; Scheffer-Teixeira et al., 2012; Scheffer-Teixeira and Tort, 2017; Tort et al., 2008; Tort et al., 2010; Xu et al., 2013). Local PAC has also been observed in human intracranial EEG (Axmacher et al., 2010; Bahramisharif et al., 2018; Canolty et al., 2006; Jiang et al., 2015; van der Meij et al., 2012; Watrous et al., 2015) and M/EEG data (Berman et al., 2015; Keitel et al., 2018; Roux and Uhlhaas, 2014) and few studies have identified inter-areal PAC in human intracranial (Chaieb et al., 2015; van der Meij et al., 2012) and M/EEG (Florin and Baillet, 2015; Park et al., 2015; Park et al., 2016). PAC is thought to reflect how sensory information processing in γ oscillations is regulated by excitability fluctuations imposed by θ and α oscillations (Canolty and Knight, 2010; Fell and Axmacher, 2011; Hyafil et al., 2015; Jensen and Colgin, 2007; Lisman and Jensen, 2013; Palva and Palva, 2012; Roux and Uhlhaas, 2014; Schroeder and Lakatos, 2009).

Another form of CFC that has been receiving increasing attention is cross-frequency phase-phase coupling, for which we introduced the term cross-frequency phase synchrony (CFS) in study **II.** Similar to phase synchrony, in CFS there exists a consistent spike-time relationship between two oscillations, but at two different frequencies f_1 and f_2, where f_1:f_2 = m:n. For example, if f_1:f_2 = 1:4, the peaks of both oscillations' phases will coincide in every fourth cycle of the faster oscillation. CFS can thus regulate neuronal communication at the speed of the higher frequency through consistent spike time relationships. In contrast, neither PAC nor AAC involve the phase of the faster oscillation; thus, these interactions operate on the slower time scale of the slower oscillation (Palva and Palva, 2012). Local CFS has been observed in human M/EEG data during rest (Besle et al., 2011; Jirsa and Muller, 2013; Nikulin and Brismar, 2006; Palva et al., 2005) and attentional and working memory (WM) tasks (Akiyama et al., 2017; Palva et al., 2005; Sauseng et al., 2008; Sauseng et al., 2009) as well as in LFPs in the rat hippocampus (Belluscio et al., 2012; Xu et al., 2013; Zheng and Zhang, 2013) and in intracranial data during WM (Chaieb et al., 2015). Inter-areal CFS has been studied in M/EEG data in rest and attentional and numeric tasks (Isler et al., 2008; Palva et al., 2005; Sauseng et al., 2008).

Less attention has been given to amplitude-amplitude coupling (AAC), in which the amplitudes of the fast and slow oscillations are coupled and phase-frequency coupling (PFC), where the frequency of the faster oscillation is modulated by the phase of the slower oscillation. AAC has been observed in neuroimaging studies (Bruns and Eckhorn, 2004; de Lange et al., 2008; Helfrich et al., 2017), but its functional relevance remains unclear, since such coupling is independent of spike time relationships per se (Palva and Palva, 2017) and PFC is difficult to study in EEG and MEG data, where instantaneous frequency peaks are

difficult to determine, although there have been studies using intracranial recordings (Ray and Maunsell, 2010; Roberts et al., 2013).

The relationship between the different forms of CFC has remained unclear; it has both been theorized that they may fulfill distinct roles, and that they are just different observable aspects of the same underlying mechanism. Different forms of CFC have been observed concurrently and there is evidence that they may interact and influence each other (Hyafil et al., 2015).

In recent years, concerns have been voiced that observations of CFC may be spurious and caused at least partially by non-sinusoidal signals (Aru et al., 2015; Cole and Voytek, 2017; Gerber et al., 2016; Kramer et al., 2008; Lozano-Soldevilla et al., 2016; Scheffer-Teixeira and Tort, 2016). Such spurious observations can arise from non-sinusoidal signals that are created by non-stationary processes leading to higher-frequency artefacts (Aru et al., 2015; Cole and Voytek, 2017; Gerber et al., 2016; Kramer et al., 2008; Lozano-Soldevilla et al., 2016; Scheffer-Teixeira and Tort, 2016; van Driel et al., 2015) or from recurring non-zero-mean sharp waveform deflections leading to spurious lower-frequency artefacts (Nikulin et al., 2007). Therefore, it is necessary to investigate whether different forms of CFC can be observed concurrently and whether they are likely to represent one underlying mechanism or two separate complementary ones; and whether it can be shown that observations of CFC represent true and not spurious interactions.

1.8 Electrophysiological neuroimaging

Neuronal oscillations can be investigated using electrophysiological neuroimaging methods, where signals are recorded with high temporal resolution (typically 600 or 1000Hz).

Magneto- and electroencephalography (MEG and EEG) are non-invasive methods of recording neuronal human brain activity. In EEG, pioneered by Hans Berger in 1924 (Berger, 1929), electrodes are attached to the human scalp that measure differences in electric potential on the surface of the head, this technique was first used. In MEG, which was first recorded by David Cohen in 1968 (Cohen, 1968), magnetic fields and field gradients outside the head are measured with magnetic coils, for which today superconducting quantum interference devices (SQUIDs) are used. (Hamalainen and Sarvas, 1989a; Hamalainen and Ilmoniemi, 1994). The electromagnetic fields and currents underlying the signals recorded with MEG and EEG are thought to be generated primarily by coherent postsynaptic currents in large sheets of co-linearly oriented pyramidal neurons (Palva and Palva, 2012).

Electrical neuronal activity can also be recorded invasively through electrodes implanted temporally or permanently in the brain. In humans, such studies are most commonly

carried out on patients with epilepsy in order to identify epileptic zones prior to surgery aiming to stop of relieve symptoms. In electrocorticography (ECoG), electrodes are places either on the dura, the outermost membrane layer surrounding the brain, or on the pia, the innermost layer. Single-or multi-contact electrodes can also be implanted deep into the cortex, cerebellum or subcortical structures in stereo-electroencephalography (SEEG, see 3.1.3) (Pesaran et al., 2018). Each of these electrodes possesses several contact points, in this manuscript referred to as channels, at which the local field potential (LFP) is recorded. The position of these can be localized using a stereotactical frame attached to the head and CT and/or MRI scans. (Cardinale et al., 2013; Pesaran et al., 2018)

With the exception of single-cell recordings, recorded electrophysiological signals always represent the activity of groups of neurons. The magnitude of these numbers scales with the recording modality, so that the time series obtained with EEG or MEG comprise a much larger number of (potentially) contributing neurons than the time series from ECoG or SEEG contacts. Further, neurons may contribute unequally to such signals, for example MEG signals are thought to be dominated by the activity of large pyramidal neurons in layers 2/3 and particularly layer 5 (Murakami and Okada, 2006; Pesaran et al., 2018).

1.9 Estimation of functional connectivity

The term functional connectivity (FC) denotes correlations between the time series of distinct sensors or brain areas, which are taken as a measure of communication between them. While in fMRI, FC is estimated as correlations of BOLD signal fluctuations, in electrophysiological neuroimaging data it can be estimated by a variety of metrics which are based on aspects of neuronal oscillations. These include spectral coherence (Nolte et al., 2004; Nunez et al., 1997), correlations of the amplitude envelope (Brookes et al., 2012; Bruns et al., 2000; de Pasquale et al., 2010; Hipp et al., 2012; O'Neill et al., 2015), or phase synchronization (Lachaux et al., 1999; Palva et al., 2005; Stam et al., 2007; Vinck et al., 2011) between neuronal oscillations of the same frequency. In MEG/EEG data analysis, volume conduction causes spurious observations of FC (see 4.1.2). Some FC metrics have been designed specifically to be less likely to report spurious connections (Colclough et al., 2016; Palva and Palva, 2012; Vinck et al., 2011), although none can alleviate the problem entirely (Palva et al., 2018). The metrics used in studies **II**-**IV** to quantify phase synchronization and amplitude correlations are described in section 3.3.1.

1.10 Estimation of directed connectivity

Measures of functional connectivity do not inform about in which direction information is transferred between connected regions. Directionality of interactions and information flow can be measured using metrics of directed connectivity. Methods used to estimate directed connectivity include Granger causality (Granger, 1969) and transfer entropy (TE) (Schreiber, 2000), which are based on information theory (Shannon, 1948) and Wiener's principle (Wiener, 1956) of observational causality. According to this principle, a signal A influences a signal B, if the future of B can be predicted better knowing the past of A, than knowing only the past of B. This can be expressed using Shannon Entropy, which quantifies the uncertainty of a signal's distribution of values. These existing implementations however have been shown to be sensitive to noise and linear mixing (Nalatore et al., 2007; Nolte et al., 2010) that occur in EEG and MEG recordings (Palva and Palva, 2012) and they have not been designed to analyze phase-specific interactions. In study **I**, we introduce Phase TE, a phase-based metric for estimating directed connectivity EEG and MEG data (see section 3.3.2).

2. Aims

Study I: The aim of this study was to develop and test Phase Transfer Entropy (Phase TE), a novel method for estimating directed connectivity among oscillations in MEG and EEG data.

Study II: The aim of this study was to investigate using source-reconstructed M/EEG data whether CFS supports the integration of synchronized networks in distinct frequency bands during visual working memory (VWM) maintenance in a match-to-sample task. We predicted that CFS if underlies the integration of sensory and executive control functions in VWM, it should be observable and dependent on VWM object load, connect task-relevant networks and predict individual VWM performance.

Study III: The aim of this study was to investigate in source-reconstructed M/EEG data if PS, CFS and/or PAC support visual attention during two multi-object tracking tasks, and are correlated with subjects' individual attentional capacity.

Study IV: The aim of this study was to investigate whether non-spurious CFS and PAC can be observed during resting state in source-reconstructed MEG and in localized SEEG data. Also, we aimed to address concerns that had been brought up about the possibility that observations of CFC might be spuriously caused by filtering artefacts stemming from non-sinusoidal or non-zero-mean signals.

3. Methods

This section describes the most important steps of data acquisition, preprocessing and analysis. More detailed descriptions are found in the method sections of the individual publications.

3.1 Data acquisition

3.1.1 Simulating Data with Neural Mass Models

We generated signal pairs with a coupled dual-kinetic 2-area neural mass model (NMM) described by David and Friston (David et al., 2004). Long-range interactions between two cortical areas (Area 1 driving Area 2) were modeled by excitatory connections between two extended Jansen models (representing each cortical area) (David et al., 2003). The model parameters were chosen to obtain relatively broadband neuronal-like signals with a power spectrum peaking in the β frequency band (15–30 Hz). Noise time series N_j with the same power spectrum as the original signals were created using frequency-domain phase shuffling (Hurtado et al., 2004) and linear mixing was simulated by linear addition of the signals.

3.1.2 Magneto- and Electroencephalography

Recordings of MEG and EEG for studies **II-IV** were carried out at Helsinki University Central Hospital. For studies **II** and **III**, MEG (204 planar gradiometers and 102 magnetometers) data and EEG data (60 channel electrode cap) were recorded concurrently (M/EEG) with a Vectorview system (Elekta Neuromag Ltd., Finland) at 600 Hz sampling rate from 12 and 19 healthy subjects, respectively. For study **IV**, MEG data (204 planar gradiometers and 102 magnetometers) was recorded from 23 healthy subjects at 1000 Hz sampling rate with a Triux system (Elekta Neuromag Ltd).

3.1.3 Stereo-Electroencephalography

For study **IV**, we also used SEEG data that had been recorded from 59 subjects affected by drug resistant focal epilepsy undergoing pre-surgical clinical assessment at Claudio Munari Epilepsy Surgery Centre, Niguarda Hospital, Milan, Italy. Anatomical positions and numbers of electrodes varied according to surgical requirements (Cardinale et al., 2013). One 10-minute set of eyes-closed resting state data was recorded from each subject with a 192-channel SEEG amplifier system (NIHON-KOHDEN NEUROFAX-110) at a sampling rate of 1000 Hz (Arnulfo et al., 2015).

3.1.4 Structural imaging

In order to localize recorded signals correctly in the brain, anatomical scans need to be recorded and co-registered with the positions of the sensors or electrodes. For MEG source reconstruction in studies **II-IV**, T1-weighted anatomical magnetic resonance imaging (MRI) scans were recorded at Meilahti hospital, Helsinki, at a resolution of 1x1x1 mm with a 1.5 T MRI scanner (Siemens, Germany). For localization of SEEG contacts in study **IV**, computertomographic (CT) scans and structural MRIs were recorded on-site after implantation (Cardinale et al., 2013; Narizzano et al., 2017).

3.2 Signal pre-processing

3.2.1 Co-registration and inverse modeling

Source reconstruction allows the reconstruction of cortical activity from measured MEG and EEG signals and the anatomical MRI images and thus can shed light on the activity of brain regions and their interactions with greater precision than sensor-level analysis. Furthermore, in connectivity analysis, source reconstruction can alleviate some of the signal-mixing problems that arise due to volume conduction and reduce the number of reported artificial connections (Palva et al., 2018; Palva and Palva, 2012). However, the computation is not straightforward, as this so-called “inverse problem” is ill-posed and has no unique solutions. Still, numerous approaches have been brought forward to obtain good estimates of neuronal activity, among them minimum-norm estimates (MNE) (Hamalainen and Ilmoniemi, 1994).

We first used Maxfilter software (Elekta Neuromag Ltd) to suppress extra-cranial noise and lo-localize recordings in signals space, and then removed ocular artefacts with independent component analysis based on the Matlab software package FieldTrip (Oostenveld et al., 2011). Source reconstruction from MEG and EEG data was performed with FreeSurfer software (Fischl, 2012) (http://surfer.nmr.mgh.harvard.edu/) for volumetric segmentation of MRI data, surface reconstruction, flattening, cortical parcellation, and neuroanatomical labeling with the 148-parcel Destrieux atlas. (Dale et al., 1999; Destrieux et al., 2010; Fischl et al., 2002). We obtained more fine-grained cortical parcellations of 200 and 400 parcels by iteratively splitting the largest parcels of the Destrieux atlas along their most elongated axis at the group-level (Korhonen et al., 2014; Palva et al., 2010; Rouhinen et al., 2013).

MNE software (http://www.nmr.mgh.harvard.edu/martinos/userInfo/data/sofMNE.php) was used to create head conductivity models and cortically constrained source models with 5000-8000 sources/hemisphere as well as for the co-localization and for the preparation of

the forward and inverse operators (Hamalainen and Ilmoniemi, 1994; Hamalainen and Sarvas, 1989b).

3.2.2 Removal of low-fidelity parcels and connections

One major confounding factor in synchrony analysis of collapsed parcel time series data are spurious edges resulting from signal mixing between neighbouring brain regions in data acquisition and source reconstruction (Palva et al., 2018; Palva and Palva, 2012). One first step to reduce spurious observations is to remove those parcels or parcel pairs where observations are the least reliable. We assessed the reliability of data based on phase correlations between real and simulated data. *Parcel fidelity* (*fid*) was defined as the phase correlation between the original true parcel time series and the forward-inverse modeled parcel time series (Korhonen et al., 2014). *Parcel cross-talk* (*ct*), was taken as the phase correlation between the forward-inverse modeled parcel time series with the original true time series of all other parcels. For each parcel, we calculated *c* as the average of *fid* values with all other parcels. *Parcel spread* (*spr*) for each parcel *p* was calculated as the mean *fid* of all other parcels with the original time series of parcel *p* and hence reveals parcels generating signals that are spuriously reflected in many other parcels. By excluding parcels with low *fid*, and high *spr*, as well as parcel pairs with high *ct* between them, the probability of spurious synchronization and anatomically misplaced connections can be reduced. These parcels are located mostly in deep and/or inferior sources, which are known to generate the least reliable signals in M/EEG and hence are most likely to incorrectly reflect signals that are generated elsewhere (Korhonen et al., 2014).

3.2.3 Frequency filtering

In order to extract the individual frequency components from the measured broadband signal, a filter is applied. In all studies, we filtered time series using Morlet Wavelets so that the filtered time series *X(t,f)* were obtained by convolution of the original time series *x(t)* with Morlet wavelets *w(t,f):* $X(t,f) = x(t) \otimes w(t,f)$ for each wavelet frequency $f_{min} \leq f \leq f_{max}$, where:

$w(t,f) = A \cdot \exp\left(\frac{-t^2}{2 \cdot \sigma_t^2}\right) \cdot \exp(2i\pi f t)$, where $\sigma_f = \frac{1}{2}\pi\sigma_t$, $A = \left(\sigma_t\sqrt{\pi}\right)^{-1/2}$, i is the imaginary unit, and the Morlet parameter m was $m = \frac{f}{\sigma_f} = 5$ (Tallon-Baudry et al., 1996). We used log-linearly spaced center frequencies ranging from 3–90 Hz, 3–120 Hz, and 1-315 Hz in studies **II**, **III**, and **IV**, respectively.

3.3 Connectivity analysis

3.3.1 Metrics of functional connectivity

Phase synchronization can be quantified using various metrics, the most common of which is the Phase Locking Value (PLV) (Lachaux et al., 1999). However, in data recorded e.g. with magnetoencephalography, volume conduction (VC) can lead to detection of artificial interactions, i.e. false positives, when the PLV is used as metric (also see 4.1.1). Other metrics only take into account the imaginary part of the signal which is not affected by VC, and are thus immune to such artificial interactions. Examples include the Phase-lag Index (PLI), the weighted Phase-Lag Index (wPLI) (Vinck et al., 2011), and the imaginary part of the PLV (Palva et al., 2018).

From a real times series *x(t)*, one can obtain the analytical time series *X(t)* can be expressed through their amplitude and phase:

$$X(t) = A(t) \cdot exp[i \cdot \theta(t)]$$

The PLV between two parcels or electrode channels *i*, *j* was estimated as:

$$PLV_{i,j} = \frac{1}{N}\left|\sum_{r,t} \exp\left[\mathrm{i} \cdot \left(\theta_i(t,r) - \theta_j(t,r)\right)\right]\right|$$

where θ_i and θ_j are the phases of the time series of parcels/channels at one frequency and $N = N_r \cdot N_t$, where N_r is the number of trials *r* and N_t is the number of samples t within a time window

The wPLI between two parcels or electrodes *i, j* was estimated as:

$$wPLI_{i,j} = \frac{\left|E\{im(X_{ij})\}\right|}{E\{\left|im(X_{ij})\right|\}}$$

where $im(X_{ij})$ is the imaginary part of the cross-spectrum of the complex time series, and $E\{\ \}$ is the expectancy value operator.

CFS at ratio 1:*m* was estimated as follows:

$$CFS_{i,j,f_1,f_2,m} = \frac{1}{N}\left|\sum_{r,t} \exp\left[\mathrm{i} \cdot \left(m \cdot \theta_{i,f_1}(t,r) - \theta_{j,f_2}(t,r)\right)\right]\right|$$

where $m = \frac{f_2}{f_1}$, where θ_{i,f_1} and θ_{j,f_2} are the respective phases of the time series of channels/parcels *i*, *j* at frequencies f_1, f_2,.

For estimation of PAC, the same formula as for CFS can be used, only the phase of the second time series is replaced with the phase of the filtered amplitude envelope time series *E(t, f_1 f_2)* that was obtained by convoluting *A(t, f_2)* with the Morlet wavelet *w(t,f_1)*: $E(t, f_1, f_2) = A(t, f_2) \otimes w(t, f_1)$. This method of estimating PAC has been shown to have small sensitivity to phase-clustering bias (van Driel et al., 2015).

PAC at ratio 1:*m* was estimated as:

$$PAC_{i,j,f_1,f_2,m} = \frac{1}{N}\left|\sum_t \exp\left[\mathrm{i} \cdot \left(\theta_{i,f_1} - \theta^{env}_{j,f_2,f_1}\right)\right]\right|$$

where θ^{env}_{j,f_2,f_1} is the phase of the amplitude envelope of the HF time series filtered with at f_1.

Cross-frequency amplitude couplings (AAC) were estimated as the Pearson correlation of the amplitude time series:

$$AAC_{i,j,f_1,f_2} = \frac{1}{N}\sum_{r,t}\left(Z_{i,f_1}(t,r) \cdot Z_{j,f_2}(t,r)\right)$$

where $(f, r, t) = \frac{A(t,r)-\mu_{t,r}}{\sigma_{t,r}}$, $\mu_{t,r} = \frac{1}{N}\sum_{t,r} A(t,r)$ and $\sigma_{t,r} = \sqrt{\frac{\sum_{t,r}\left(A(t,r)-\mu_{t,r}\right)}{N}}$.

In studies **II** & **III**, these estimations were carried out over short time windows (0.3 and 0.5 s, respectively) prior to and past stimulus presentation. In Study **IV**, estimations were carried out over the whole recorded time of about 10 minutes.

3.3.2 Estimating directed connectivity with PhaseTE

The uncertainty of a variable *X* is defined by its Shannon Entropy $H(X) = -\sum_x p(x)\log \mathrm{p}(x)$. Shannon entropy of a variable at a given time point can conditioned on another variable, or on itself at a different time point:

$$H(Y(t), Y(t')) = -\sum p(Y(t), \mathrm{Y}(t'))\log\ p(Y(t), Y(t'))$$

The Transfer Entropy from a signal *X* to another signal *Y* can be expressed as the difference between the Shannon Entropy of the present of Y (*Y(t)*) conditioned on its past (*Y(t')*) and the Shannon Entropy of the present of *Y* conditioned on both its past and the past of *X* (Schreiber, 2000)*:*

$$TE_{X\to Y} = H(Y(t)|Y(t')) - H(Y(t)|Y(t'), X(t'))$$

In study **I**, we introduced a new measure of directed connectivity named Phase Transfer Entropy (Phase TE). In Phase TE, entropy is estimated not from the signals *X*, *Y*, but instead from their phases θ_x, θ_y. Accordingly, Phase TE for a given analysis lag δ is defined as:

$$Phase\ TE_{X \to Y} = H\big(\theta_y(t), \theta_y(t')\big) + H\big(\theta_y(t'), \theta_x(t')\big) - H\left(\theta_y(t')\right) - H\big(\theta_y(t), \theta_y(t'), \theta_x(t')\big)$$

where $\theta_x(t')$ and $\theta_y(t')$ are the past states at time point $t'=t-\delta$: $\theta_x(t') = \theta_x(t-\delta)$ and $\theta_y(t') = \theta_y(t-\delta)$).

The probabilities necessary for the estimation of TE can be obtained by estimating the state-space of the processes underlying time series. This is explained in more detail in the methods section of study **I**.

3.3.3 Statistical testing

In study **II**, statistical significance of connections in was estimated on the group level by comparing values during VWM maintenance to those in the pre-stimulus period using a two-sided t-test, or correlating them with object load using Pearson's correlation test. We then removed as many positive significant findings as predicted by the alpha-level to be false discoveries to compensate for multiple comparisons and to reduce false discovery rate (FDR). In study **III**, significant correlation with load was estimated by a Pearson randomization test. In addition to the correction performed in study **II**, we also estimated a FDR-adjusted threshold for the number of significant observations that could be expected to arise by chance from graphs of random *p*-values after the false discovery reduction in any single frequency of all wavelet frequencies. In study **IV**, significance was established by comparing observed values of interaction strength and connection strength to values obtained using surrogates which were created at the single-subject level by shifting one of the time series by a random number of samples. The expected chance level of connection density was subtracted from reported values.

3.3.4 Network analysis and visualization

Networks can be characterized and analyzed using graph theory (Bullmore and Sporns, 2009). In doing so, brain regions, e.g. cortical parcels, are the nodes of a network, and the interactions/connections between them are the edges. There are several ways in which networks can be constructed: Edges can be either binary, taking only values of 0 and 1, or weighted, representing the strength of the interaction. A network in which some edges are non-existent, i.e. have a value of 0, is called a sparse network. By retaining only edges which either are above a certain strength level or alternatively are found to be significant in statistical tests, sparse networks can be obtained and can then be characterized by the

connection density *K*, that is the number of existing edges divided by the number of possible edges. An individual node can be characterized e.g. by its degree, i.e. the number of adjacent edges, by its relative degree, i.e. the number of adjacent edges divided by the maximum possible number of adjacent edges, or by its centrality, i.e. how many of the shortest paths between other nodes pass through it. Nodes with high degree and/or centrality are called hubs and considered important for communication within networks and their stability.

In studies **II-IV**, we used graph theory to characterize network structure through connection density and hubs, and in study **IV** introduced a new node metric that represented the preferred directionality of nodes in CFC interactions.

In study **II**, we performed several further analyzes on the networks spanned by significant CFS connections. In order to test whether CFS between two frequencies f_1 (LF), f_2 (HF) connected PS networks at these frequencies, we tested whether the degree of LF and HF frequency hubs of CFS networks was correlated (Pearson's correlation test) with their degree in LF and HF PS networks. Further, we visualized the major nodes and edges of networks as graphs drawn on flattened cortical surfaces, using a novel hyperedge bundling technique for improved visualization of CFS connections and minimization of the number of 2^{nd} order spurious connections (Wang et al., 2018). Finally, to establish functional significance of CFS, we estimated the correlation (Pearson's correlation test) of inter-individual variability in the summed strength of these networks with the variability in VWM capacity, which was obtained from their hit rates at different object loads.

4. Results

Study I: Phase transfer entropy: A novel phase-based measure for directed connectivity in networks coupled by oscillatory interactions

In this study, we explored phase transfer entropy (Phase TE) as a metric of directed connectivity among neuronal oscillations. Transfer entropy (TE), based on information theory, estimates whether the future of a time series A can be predicted better knowing both its past and the past of another time series B than from only A's past alone; if so, then time series B is found to causally influence signal A. Phase TE quantifies the transfer entropy between phase time-series such as those obtained by narrow-band filtering neuronal time series. We simulated data with coupled Neuronal Mass Models to both evaluate the characteristics of Phase TE and compare it to of a real-valued TE implementation. In order to determine directionality between two signals, differential Phase TE was computed as the difference of the Phase TE values in both possible directions. Differential Phase TE increased monotonically with coupling strength and correctly detected direction for coupling strengths > 0 (Figure 2).

We found that our metric reliably detected strength and direction of coupling across a wide range of parameters, such as analysis lag, samples size, noise and linear mixing, as can be observed in real MEG and EEG recordings, and did so more robustly than real-valued broadband or narrowband TE implementations (Figure 3). Further, Phase TE was shown to be more computationally efficient than those implementations. We also found that appropriate null-hypothesis distributions can be obtained from surrogate data for estimation of statistical significance.

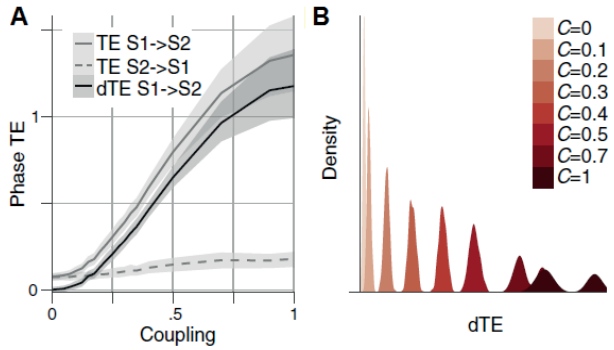

Figure 2: Differential Phase TE correctly detects coupling direction and increases with coupling strength (A) and distributions of differential Phase TE for different coupling values showed only small overlap (B). Adapted from study II.

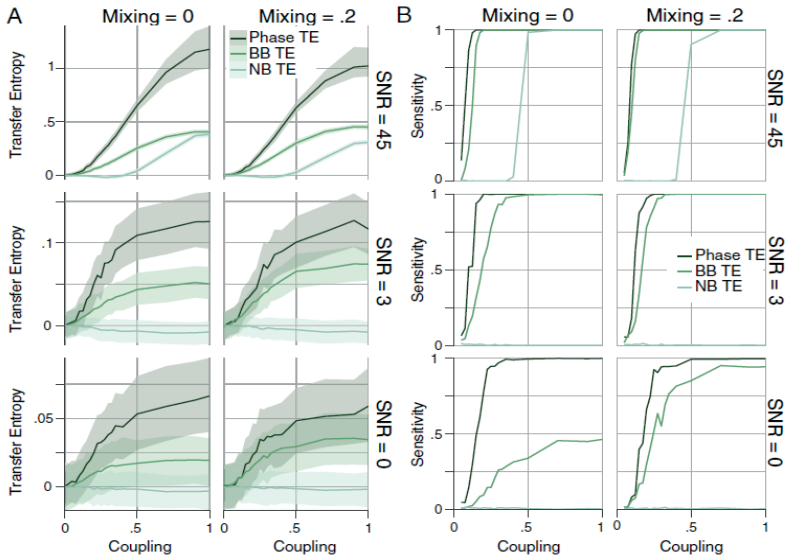

Figure 3: Differential Phase TE detects directed interactions more reliably than differential broadband (BB) or narrowband (NB) real-values Transfer Entropy across different values of SNR and mixing, which is evident both in absolute values (A) and in sensitivity estimations (B). Adapted from study II.

Study II: Cross-frequency synchronization connects networks of fast and slow oscillations during visual working memory maintenance

In this study, we analyzed neuronal data recorded with concurrent M/EEG from healthy subjects performing a visual working memory (VWM) task (see Figure 4). We hypothesized that inter-areal CFS would support integration between the frontoparietal α networks and occipitoparietal β and γ sensory networks during VWM maintenance and thus predict VWM performance. We estimated *n:m* inter-areal cross-frequency phase synchrony (CFS) among cortical parcels in source-reconstructed data during the VWM retention period (from 0.4 s after stimulus presentation), in which there is no confound by stimulus-evoked activity. We found that inter-areal CFS could be observed among cortical parcels (Figure 4) was modulated by task and showed distinct patterns across frequencies and ratios (Figure 5A-D).

Connection density of inter-areal CFS was increased between high-θ (5-8Hz) and α–γ and between high-α (11-15Hz) and β–γ frequencies at CF ratios from 1:2 to 1:9 in a harmonic structure. Increases in CFS between high-α (10-15 Hz) and higher frequencies were also correlated with VWM load at ratios 1:2 – 1:4, indicating relevance of CFS for VWM maintenance. CFS between low- α (7-10 Hz) and higher bands was decreased at ratios 1:2 – 1:9. We also estimated inter-areal phase-amplitude coupling (PAC) similarly to CFS. Inter-areal PAC was increased among θ, α and β bands at ratios 1:2 and 1:3, showing a spectral pattern markedly distinct from that of CFS (Figure 5E-H).

To verify that observations of CFS weren't caused by changes in signal-to-noise ratio (SNR), we estimated the SNR from comparisons of experimental and empty-room recordings and verified that only a small fraction of CFS could potentially be explained by changes in SNR. Further, we tested whether variance of changes of CFS-PLV were correlated with amplitude and found no overall correlation. Finally, to rule out that CFS was caused by non-sinusoidal waveforms, we computed cross-frequency amplitude-amplitude correlations, which showed a different structure from CFS, with no harmonic pattern over low frequencies.

Increased CFS was observed especially among visual, fronto-parietal, and dorsal attention networks. LF network hubs in α and θ bands that showed increased numbers of CFS connections during the VEM maintenance were found mainly in regions belonging to the fronto-parietal, dorsal, attention and ventral attention networks, notably including prominent hubs in the right PPC, whereas HF hubs were localized mainly to visual regions and parts of the dorsal attentional networks. Hubs that were less active during VWM maintenance were localized to default and somatomotor networks, which are not thought to be involved in VWN. We also computed the correlation of vertex degree between LF and HF hubs in CFS and the vertex degree in PS networks at the same frequencies. We found that indeed, these values were correlated, supporting the hypothesis that PS networks in different frequency bands are connected by CFS.

Finally, we found that inter-individual variability in the strength of CFS networks in ratios 1:2 – 1:5 over high-α band and in ratios 1:6 – 1:9 over high-θ band predicted intra-individual variability in VWM capacity, indicating that CFS is behaviourally relevant for VWM. No such relationship was found for PAC.

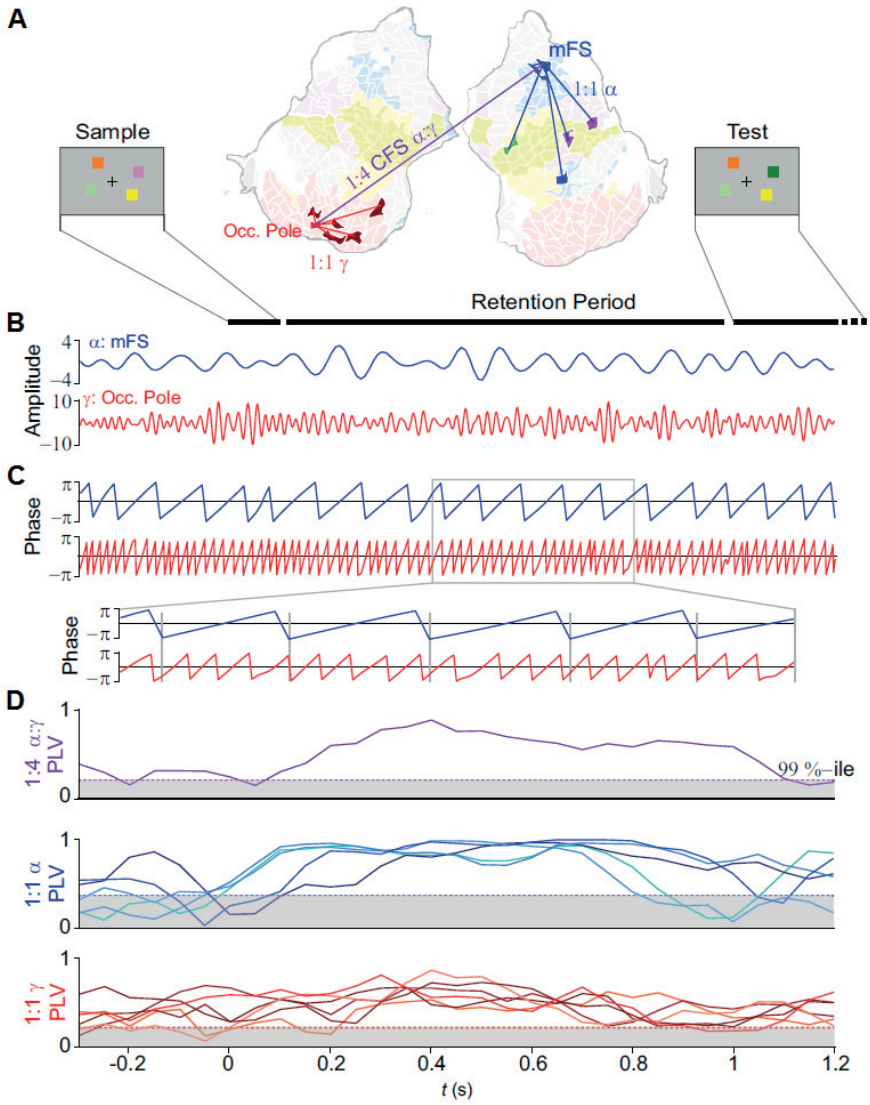

Figure 4: Inter-areal cross-frequency phase synchrony (CFS) in human cortex is modulated during a visual working memory task. A) Illustration of the delayed-match-to-sample experimental paradigm. The sample stimulus containing 1–6 colored squares is presented for 0.1s and then after a 1s retention period a test stimulus appears and the subject responds whether one of the objects has a different color than in the sample stimulus. The flattened cortical surface shows an example of 1:4 CFS (purple line) connection between α (13 Hz) oscillations in the right medial frontal sulcus (MFS) with γ (54 Hz) oscillations in left occipital pole (Occ.Pole) during VWM retention. These α and γ oscillations were concurrently also 1:1 synchronized in networks of other cortical areas (blue and red lines, respectively). B) The α and γ narrowband time series. C) The phase of the narrowband signals, with the zoom-in illustrating CFS during the retention period. D) Strength of CFS (top) and of α and γ phase synchrony (middle and bottom). The grey area denotes the 99%-ile confidence intervals of null hypothesis PLV values obtained with time-shifted surrogate data. From study ***II****.*

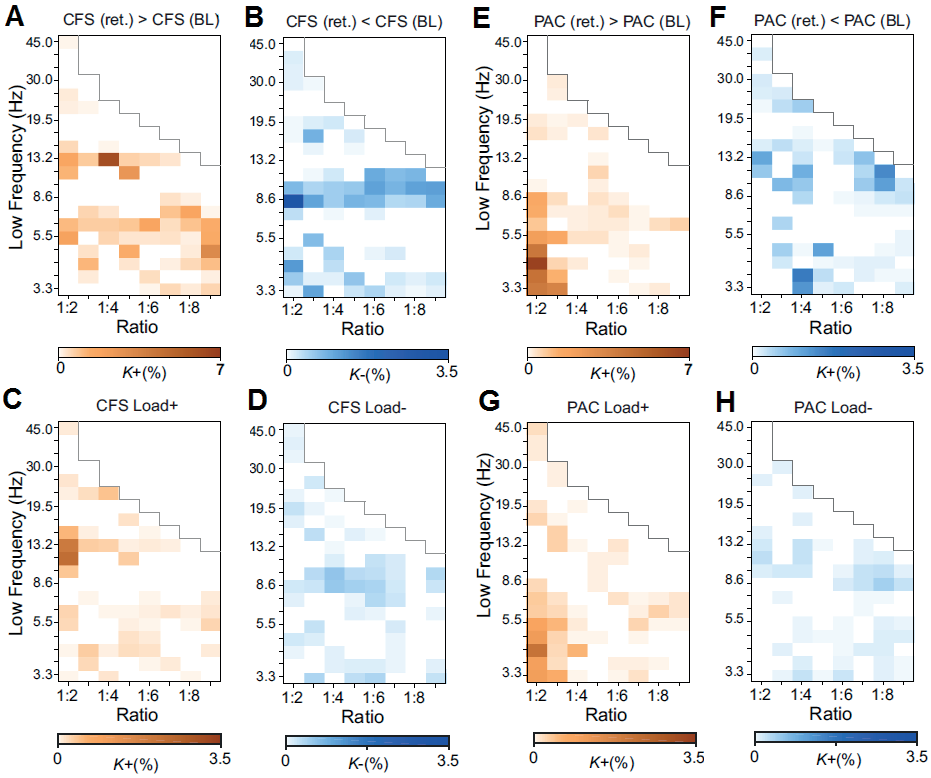

Figure 5: During VWM retention, inter-areal cross-frequency phase synchrony (CFS) was enhanced across ratios over higher θ and higher α band and suppressed over lower α and lower θ band. K+ and K- indicate fractions of inter-areal CFS connections that were significantly stronger (A) or weaker (C) during VWM maintenance than in pre-stimulus baseline; or that were positively (B) or negatively (D) correlated with VWM load. Inter-areal Phase-Amplitude Coupling (PAC) was stronger than during baseline (E) at low ratios in θ band and across ratios in high θ, suppressed over α band across ratios and for medium ratios over low θ (F). Positive correlations of PAC with load (G) showed similar profile to E, while negative correlations were comparatively weak (H). Adapted from Study ***II****.*

Study III: Distinct spectral and anatomical patterns of large-scale synchronization predict human low and high attentional capacity

In this study, we investigated the role of phase-synchronization and CFC in setting the capacity limits of visual attention. To this end, we analyzed source-reconstructed M/EEG data from healthy subjects performing two multi-object tracking (MOT) tasks which are commonly used to study attentional capacity limitations (Bettencourt et al., 2011; Oksama and Hyona, 2004; Pylyshyn and Storm, 1988). In the task, we varied the number of attended of visual objects between one and with a maximum of four objects. The visual objects were presented either without (T1) or with (T2) the presence of differently colored distractor among the targets (see Figure 6). We then estimated phase synchrony and CFS and PAC networks for frequencies from 3–120 Hz and for all cortical parcels of the source-reconstructed MEG data.

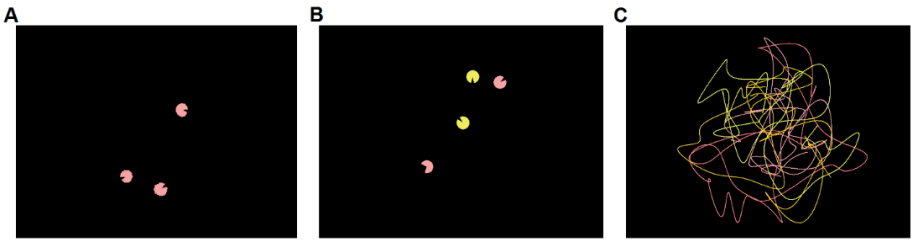

Figure 6: Multi-object tracking tasks. A) Task 1, with 3 out of possible 4 objects moving on the screen. B) Task 2, with two target (pink) and two distractor (yellow) objects. C) Example paths of target and distractor objects over a 45 second period. Adapted from Study ***III.***

We found that PS in α band (T1&T2) and in low-γ band (Lγ, 30-60 Hz) in T1 and in high-γ band (Hγ, 60-120 Hz) in T2 preceding the target event was stronger for correct target detection. Further, PS was positively correlated with attentional load in θ and Hα bands in T1 and with low-α and Hγ bands in T2. When subjects were divided into two groups based on their attentional capacity, significant different spectral patterns of PS were observed in multiple frequency bands.

We further observed significant inter-areal CFC to be correlated with task performance. In both tasks, α:β, α:γ, β:γ and Lγ:Hγ coupling were observed across many ratios, but after correcting for false discovery rate only β:γ and Lγ:Hγ 1:2 CFS in T2 remained. Importantly, visual inspection implicated that CFS differed between high- and low-capacity subjects. Notably, β:γ and Lγ:Hγ 1:2 CFS was stronger at higher frequencies for high-capacity subjects than low capacity subjects, however these results were significant in a group permutation test for only few individual frequency ratios. (Figure 7A-B). In addition to CFS, we also observed significant inter-areal PAC that connected α, β and γ bands at ratios 1:3 – 1:6 (T1)

and 1:2 – 1:8 (T2) for high-capacity subjects that was largely absent in subjects with low capacity (Figure 7C-D). Importantly, these findings were found to be significant in group permutation testing for a number of frequency ratios.

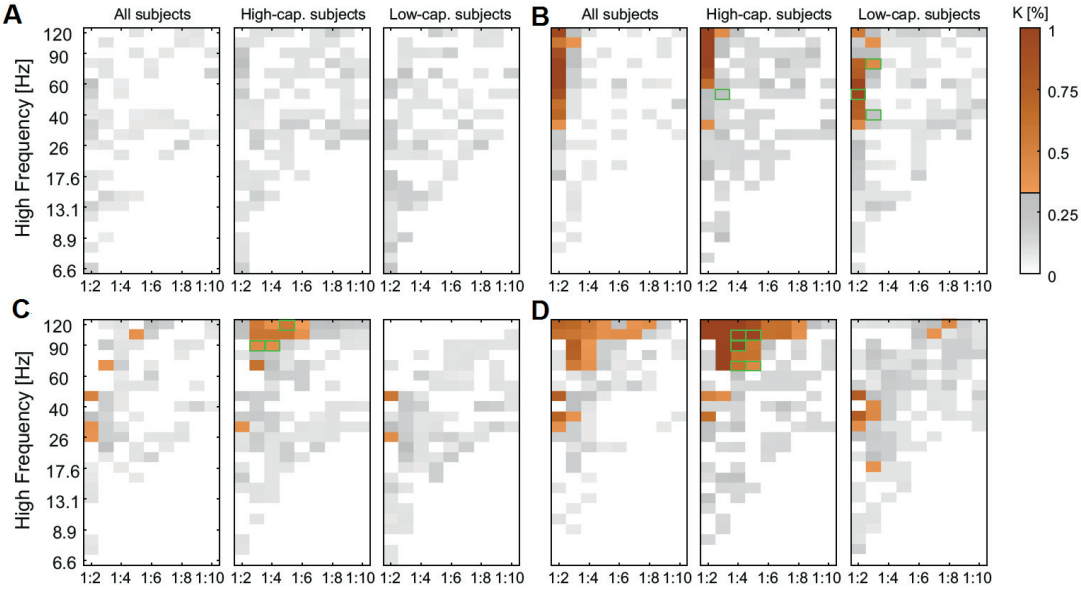

Figure 7: Connection Density (K) of inter-areal CFS connections whose strength was positively correlated with load in (A) T1 and (B) T2 (Pearson's randomization test across loads 2-4). Values are shown in color-scale when p < 0.05 and when K was > 0.33%, and in grayscale when p < 0.05 but K < 0.33%, with 0.33% representing the FDR-adjusted threshold for significant K values. Inter-areal PAC coupled the phase of β and low-γ band oscillations with high-capacity subjects at ratios 1:3 - 1:6 in T1 (C) and at ratios 1:2 - 1:8 in T2 (D). Green outlines show where group differences between high- and low-capacity subjects were found to be significantly different in a group permutation test (N=200). From study ***III****.*

Study IV: Inter-areal CFS and PAC in human resting state

In this study, we aimed to identify if true, non-spurious inter-areal CFS and PAC, characterize human resting state activity. We analyzed SEEG data from 59 epileptic patients and source-reconstructed MEG data from 23 healthy subjects. We estimated PS, and both local and inter-areal CFS and PAC at ratios 1:2 – 1:7 from both MEG and SEEG data. We observed robust inter-areal α:β and α:γ CFS and PAC at ratios 1:2 and 1:3 in both MEG and SEEG data. In SEEG data, also δ/θ:α CFS at these ratios and higher-ratio θ/α:γ PAC were observed Further, coupling between γ and very high γ (>120 Hz) was observed in MEG data at rations 1:2 and 1:3 for CFS and 1:2 – 1:7 for PAC (Figure 8). Also, local CFS and PAC were observed that showed similar profiles to inter-areal CFC, but at generally higher connection densities. However, for local CFC, spurious observations can not be distinguished from true ones.

We addressed concerns that observations of CFC may be spurious if they are caused by non-sinusoidal waveforms that are erroneously interpreted as two different processes. We posited that for inter-areal CFC, it is possible to show that the two processes between which true CFC is observed are separate and not otherwise connected, proving that they are true and not spurious; and implemented a method to identify non-spurious connections in our data. We removed CFC connections between two narrowband signals at different locations if these were also connected by local CFC and PS, and thus could not be safely assumed to be independent. Even after removal of possibly spurious observations, connection density remained above chance level (Figure 8) for most observed interactions. The observed coupling between γ and very high γ in MEG data however was reduced to near zero, which together with the absence of such coupling in SEEG data pointed at an artefactual origin of these observations. For local CFC, no correction for spurious connections could be done and thus it remains unclear how many of these observations represent true CFC.

We further found in both datasets that connection density of inter-areal CFC was higher among short-range connections than long-range ones and in superficial than deep cortical layers. Finally, using graph-theory based metrics, we identified low- (LF) and high-frequency (HF) hubs for all interactions. We found that in both datasets, LF hubs in CFS were mainly localized to lateral prefrontal and medial parietal cortex and HF hubs in posterior parietal, somatomotor and temporal cortex, whereas for PAC, the localization was opposite to that of CFS (Figure 9). Similar results were found when using a directionality analyses that provided an alternative way of identifying LF and HF hubs.

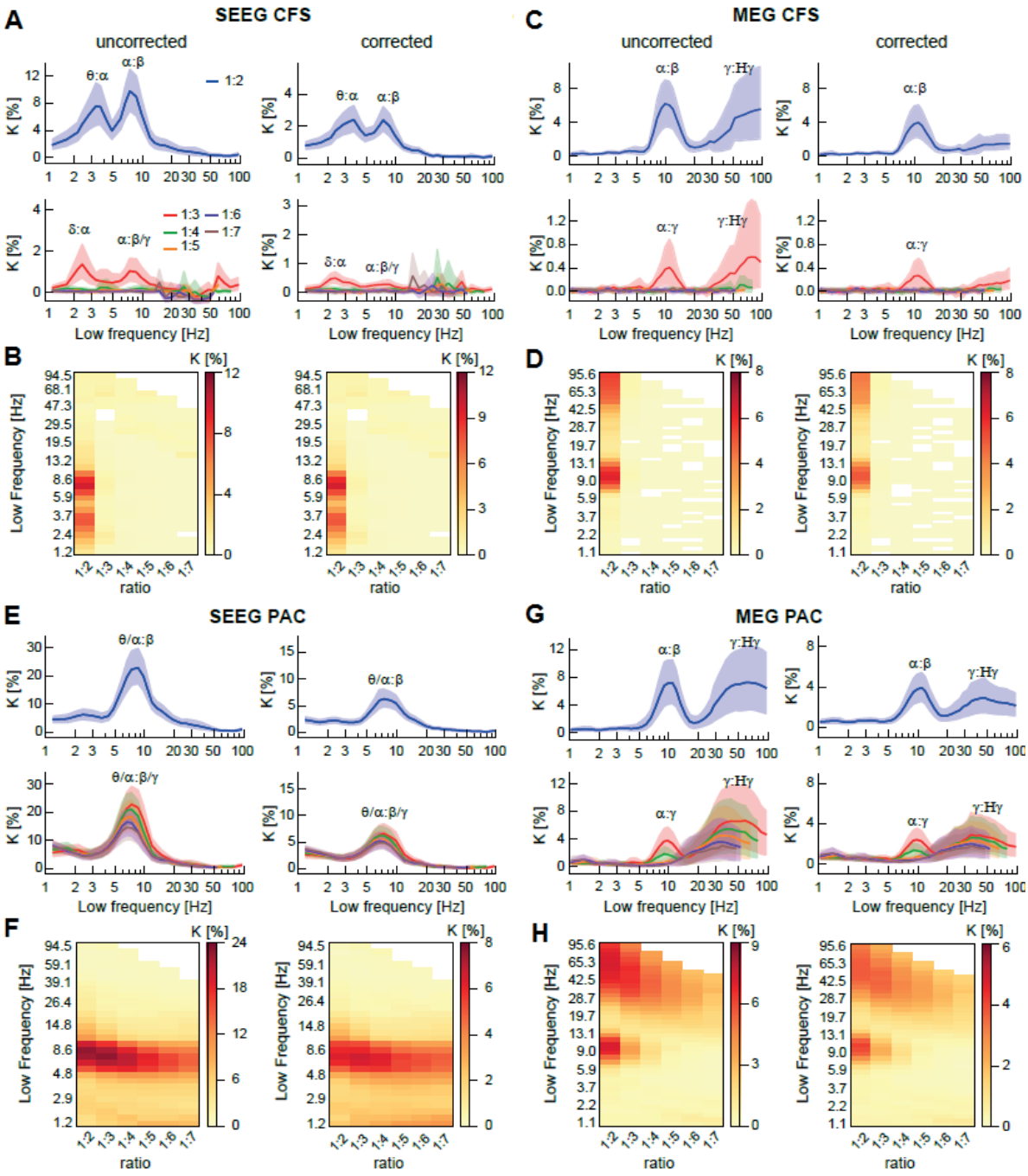

*Figure 8: Cross-frequency synchrony (A-D) and phase-amplitude coupling (E-H) in SEEG resting state data from epileptic patients and source-reconstructed MEG resting state data from healthy subjects. Mean connection density values K are given before and after removal of potentially spurious connections. A and B show the same mean values, in A 95% confidence limits are added (colored area); the same applies to (C,D), (E,F) and (G,H). Prominent peaks are noted with the frequency bands they connect. From study **IV**.*

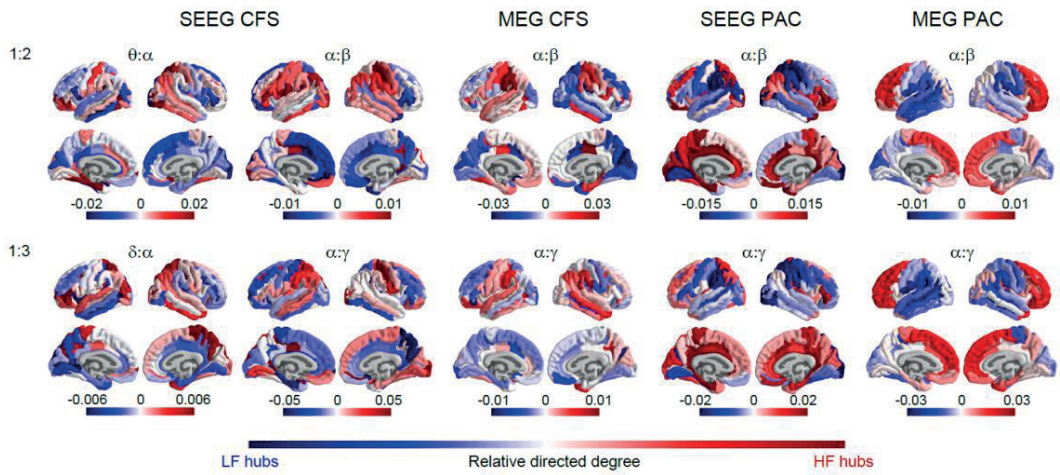

Figure 9: Relative low (f1) vs. high (f2) degree of each brain region (parcel) for CFS and PAC networks. Relative degree values indicate whether parcel is primarily a hub for the low frequency (f1, red) or high frequency (f2, blue) in inter-areal CFC. Top row: Brain anatomy of CFS and PAC at ratio 1:2 connecting θ:α and α:β frequencies. Bottom row: Brain anatomy of CFS and PAC networks at ratio 1:3 connecting δ:α and α:γ frequencies. CFS and PAC networks show nearly opposite anatomical structures connecting anterior and posterior brain regions.

5. Discussion

In this thesis work, two main questions were investigated, namely how information flow in phase-synchronized networks can be measured, and how such networks are integrated across frequency bands.

In study **I**, we introduced a novel metric of directed connectivity, Phase TE and tested and confirmed its suitability for the analysis of electrophysiological neuroimaging data using simulated data generated with neural mass models.

In studies **II-IV**, we investigated in electrophysiological neuroimaging data whether two forms of cross-frequency coupling (CFC), namely phase-amplitude coupling (PAC) and phase-phase coupling or cross-frequency phase synchrony (CFS) could be observed in the human cortex during task and rest. We showed in study **II** that inter-areal CFS and PAC are observed during visual working memory (VWM) maintenance and that inter-areal CFS was functionally relevant and correlated with subjects' VWM capacity. In study **III**, we found that inter-areal CFS and PAC supported visual attention in two multi-object tracking tasks. In study **IV**, we observed inter-areal CFS and PAC during the human resting state and used a novel graph-based method to confirm that observations reflected true and not spurious interactions and found diverging anatomical distributions for CFS and PAC.

5.1 Phase Transfer Entropy as a novel method for estimating directed connectivity

In Study **I**, we showed that Phase TE is an appropriate and efficient model for investigating directed connectivity in MEG and EEG data. In the analysis of simulated data, Phase TE detected strength and direction of connectivity between signal pairs, also for low coupling strengths, and in the presence of realistic amounts of noise and mixing. Compared to non-phase-based transfer entropy, Phase TE showed superior computational efficiency and superior performance in detecting direction of information flow among linear mixing and noise. Therefore, Phase TE shows great promise for the investigation of information flow in M/EEG data.

5.2 Inter-areal cross-frequency coupling characterizes neuronal activity in the human cortex

The studies **II-IV** presented in this thesis have investigated two forms of inter-areal cross-frequency coupling, namely phase-amplitude coupling (PAC) and phase-phase coupling or cross-frequency phase synchrony (CFS).

While cross-frequency coupling has been investigated for two decades, more attention has been given to PAC than CFS and more studies have investigated local CFC than inter-areal CFC. Of those inter-areal studies, only few were carried out with source-reconstructed M/EEG data (Florin and Baillet, 2015; Park et al., 2015; Park et al., 2016) or intracortical recordings (van der Meij et al., 2012).

In study **II**, we set out to show that task-relevant increases in inter-areal CFS could be observed during a VWM task in source-reconstructed M/EEG data and that they were different from inter-areal PAC and related to individual capacity, which was corrobated by the results. In study **III**, we investigated both inter-areal CFS and PAC with source-reconstructed M/EEG during two visual attention tasks and found task-relevant increases for both and different spectral patterns between subjects with low and high attentional capacity, indicating that CFC plays a crucial role for visual attention. In study **IV**, we showed that inter-areal CFS and PAC also characterize the human resting state, using both source-reconstructed MEG and SEEG data. Both CFS and PAC resting-state networks showed similarities to known within-frequency resting state networks. We also estimated local CFC in this study, which showed similar peaks, but was significant for a higher fraction of parcels than the fraction of parcel pairs in inter-areal CFC. However for local CFC, spurious and true observations can not be disentangled, unlike inter-areal CFC (see 5.5).

These findings extend previous reports of inter-areal CFC (Florin and Baillet, 2015; Palva et al., 2005; Park et al., 2014; Park et al., 2015; Schack et al., 2005; van der Meij et al., 2012), providing further support for the existence and functional relevance of CFC in the human brain.

5.3 The role of CFC in VWM and attention

Visual working memory and visual attention are two closely related cognitive functions that are supported by activity in several regions distributed across the cortex, especially in the frontal, posterior parietal and occipital cortices. Several studies have found that representation of visually perceived and attended objects is localized in the occipital cortex (Emrich et al., 2013; Riggall and Postle, 2012; Sreenivasan et al., 2014) and there enabled by

γ oscillations (Busch et al., 2006; Honkanen et al., 2015; Michalareas et al., 2016; Rouhinen et al., 2013; Vidal et al., 2006) and attended stimuli (Rouhinen et al., 2013; Vidal et al., 2006). The frontoparietal network, including the lateral prefrontal cortex (PFC) and posterior parietal cortex (PPC) has been shown to underlie regulation, manipulation and utilization of objects stored in VWM (Harding et al., 2015; Markowitz et al., 2015; Rowe et al., 2000; Sreenivasan et al., 2014) and attention by means of θ and α connectivity (Doesburg et al., 2016; Doesburg et al., 2009; Lobier et al., 2017; Siegel et al., 2008).

In studies **II** and **III**, we set out to investigate whether CFC could underlie the integration of oscillations and PS networks across regions and frequency bands to support VWM and visual attention, respectively. In study **II**, we found that inter-areal CFS of θ and high-α (10-15 Hz) bands with harmonic higher frequencies was elevated during VWM maintenance period compared to pre-stimulus baseline and also correlated with object load. We visualized significant edges and the main hubs that they connected, and found that low-frequency (LF) hubs in θ and high-α were localized mainly in prefrontal and parietal regions, that are part of the frontoparietal control network and the ventral and dorsal attention networks. High frequency (HF) hubs in γ band were found especially belonging in regions to the dorsal attention network as well as in occipital regions and some regions of the frontoparietal network. We further wanted to analyze whether CFS connected PS networks and found that vertex degree, which indicated network hubs, was correlated between LF and HF hubs in CFS and hubs in PS networks of the corresponding frequencies, and that central hubs included the PPC and frontal regions in θ and high-α networks. HF hubs in the γ band were found in the occipital regions and the inferior temporal gyrus, which is associated with object recognition and representation. These results indicate that CFS in is indeed important for VWM and connects PS networks of different frequency bands. Increases in inter-areal PAC and correlations with object load were also found, but mostly of the low θ band with higher frequencies. Also, we found that inter-individual variability in CFS network strength of high-α and higher frequencies at ratios 1:2 – 1:5 and of θ band and higher frequencies at ratios 1:6 – 1:9 predicted intra-individual variability in VWM capacity, indicating that CFS is behaviourally relevant for VWM. No such relationship was found for PAC.

In study **III**, we found that inter-areal CFS among β, low γ (Lγ, 30-60 HZ) and high γ (Hγ, 60-120 Hz) at ratios 1:2 and 1:3 in T2 was correlated with load at values of connection density surpassing the FDR-adjusted threshold. Findings in task 1 (T1) and at other ratios in task 2 (T2) did not reach significance after controlling for false discovery rate (FDR). Inter-areal PAC connected α, β, Lγ and Hγ bands in both tasks. Findings of CFC at other ratios did not surpass the FDR-adjusted *K* threshold. Notably, in this study overall connection density

values were small compared to the other studies, which may have been influenced by the choice of a more fine-grained cortical parcellation or the statistical methods. Analysis of PS in that study showed that successful target detection was associated with α synchrony between regions in frontoparietal and attentional networks for T1 and in frontoparietal and visual regions for T2, and for both tasks, with γ synchrony between prefrontal and occipital regions. Also, θ synchrony between occipital and frontoparietal regions was correlated with object load for both tasks.

The results from study **II** imply that CFS connects the integration of attentional and representational processing in VWM in a role complementary to that of PAC. In study **III** there were only sparse confirmed observations of CFS and of PAC among β and γ bands, and observations of θ:α–γ and α:β–γ CFC were too sparse to pass the adjusted *K* threshold. Nevertheless, these findings along with those of PS in the same study, which showed θ, α and γ synchrony among frontoparietal, attentional and occipital regions, and the fact that the observed CFS and PAC differed between low- and high-capacity groups, imply that CFS and PAC also support for visual attention in a manner similar to VWM.

5.4 CFS and PAC are distinct complementary processes

Another question that has remained open is whether CFS and PAC constitute separate mechanisms or are just different aspects of one underlying mechanism. In studies **II-III**, the spectral profiles of task-related increases and decreases in CFS and PAC were found to be different from each other. Further, in study **II** variability in CFS but not PAC network strength was correlated with variability in individual VWM capacity, whereas in study **III**, we observed differences in spectral profiles between low- and high-capacity subjects in both PAC and CFS, but at different frequency ratios. Results from study **IV** indicate that both CFS and PAC also characterize the human resting state, but with differing profiles. In that study, α hubs of CFS were observed mostly in frontal-medial regions belonging to default, control and attentional networks and β and γ hubs mostly in more posterior regions such as sensorimotor, temporal and occipital cortices, whereas the pattern for PAC was opposite to that; for both, patterns were consistent across MEG and SEEG data. These results together strongly imply that CFS and PAC are indeed distinct mechanisms likely fulfilling different complementary roles.

5.5 True observations of inter-areal cross-frequency coupling

One common critique that has been brought up is that observations of CFC might be spurious, caused by increases in SNR during task, or by non-sinusoidal or non-zero mean waveforms (Aru et al., 2015; Cole and Voytek, 2017; Gerber et al., 2016; Jones, 2016; Kramer et al., 2008; Lozano-Soldevilla et al., 2016; Scheffer-Teixeira and Tort, 2016).

In study **II**, we performed a number of tests to rule out that the possibility that inter-areal CFS might be caused by non-sinusoidal waveforms or changes in amplitude and/or SNR. These tests showed that only a small fraction of observed significant CFS connection could possibly be explained by these causes, supporting the interpretation that these observations indeed reflect true dynamic cross-frequency coupling of neuronal oscillations and are not caused by spurious interactions.

In study **IV** we also addressed concerns about the possibility of CFC observations being spurious and caused by non-sinusoidal waveforms or linear fast components (Aru et al., 2015; Gerber et al., 2016; Lozano-Soldevilla et al., 2016) or non-zero mean signals (Nikulin et al., 2007). In these cases, CFC would be measured between components in different frequencies stemming from the same single process. True CFC however connects two otherwise independent processes, and while it is not possible to prove the existence of such in local CFC, it is possible for inter-areal CFC. Inter-areal CFC can only be spurious when the two signals are otherwise connected, via local CFC and within-frequency (1:1) PS. We developed a graph-based method to remove all possibly spurious connections and showed that for both inter-areal CFS and PAC the connection density in all major peaks remained above zero even if all possibly spurious connections were removed. Further, the results of this study were also strengthened by the consistency of results between SEEG and MEG datasets.

The results from both study **II** and **IV** therefore provide strong support for the existence of true inter-areal CFC in both task and resting state.

5.6 Similarities and differences between task and resting state

Having established that inter-areal CFC characterizes VWM and visual attention as well as the resting state, one important question is whether the observed patterns are similar to each other across studies, which would support the fundamental importance of CFC for cognitive function.

In study **II,** inter-areal CFS was found to be enhanced during VWM retention above baseline and correlated with load for θ:α–γ at ratios 1:2-1:9 and Hα:β–γ (Hα: high α, 10-15 Hz) at

ratios 1:2-1:7. Also, β:γ CFS was observed at low ratios. In study **III**, which investigated visual attention, we observed that inter-areal β:γ and γ:γ and possibly α:β and α:γ coupling were correlated with visual object load. Finally, in study **IV**, we observed significant α:β and α:γ inter-areal coupling at ratios 1:2 and 1:3 in both SEEG and MEG data, and additionally δ/θ:α coupling at the same ratios in SEEG data.

Inter-areal PAC was observed in study **II** to be enhanced above baseline and correlated with load between θ and α–γ bands, with strongest *K* values for low frequencies around 4Hz and ratio 1:2. Notably however, for low frequencies of 6-8 Hz, i.e. at the border of θ and α band, PAC was observed at all computed ratios up to 1:9. In study **III**, we observed α:β, α:γ, β:γ and γ:γ coupling correlated with visual object load. In study **IV**, we observed α:β–γ coupling and γ:Hγ coupling at ratios 1:2 – 1:4 in MEG data and, and θ/α:β–γ coupling at all computed ratios 1:2 – 1:7 in SEEG data.

Together, these results imply that both inter-areal CFS and PAC are present in resting state and modulated by task. Although it should be noted that absolute values of the connection density *K* can not be compared directly between these studies because the different used cortical parcellations and statistical methods, nevertheless the observations of similar frequency ratios in these studies is worthy of emphasis. The most consistent findings across resting state and the investigated tasks were that of 1:2 α:β CFS and of θ/α:β–γ PAC across multiple ratios. Other observed frequency ratios, like α:γ CFS and θ:α–γ CFS during VWM maintenance in study **II**, or β:γ and γ:γ CFS and PAC during the execution of multi-object tracking tasks in study **III**, indicate that certain frequency combinations may be recruited dynamically during task. Also, in study **IV**, θ/α:γ PAC at higher ratios was observed in SEEG data. Such PAC is similar to many previous findings of high-ratio θ:γ ratios in the rat hippocampus (Belluscio et al., 2012; Scheffer-Teixeira et al., 2012; Tort et al., 2008; Tort et al., 2010) and in human intracranial recordings (Axmacher et al., 2010; Bahramisharif et al., 2018; Canolty et al., 2006; Chaieb et al., 2015; van der Meij et al., 2012), but might not be observable in MEG and EEG recordings because it connects only smaller populations.

Together, these findings point towards a universal role for CFC in the integration of neuronal activity distributed across frequency bands to enable cognition that is dynamically modulated by task demands.

5.7 Outlook

In study **I**, we introduced Phase TE as a metric for directed connectivity and tested its suitability using simulated data that was made to realistically recreate properties of real EEG and MEG neuroimaging data. We expect that Phase TE will also prove useful in the actual analysis of such data, which is to be carried out in future studies.

In studies **II**-**IV**, we showed that true inter-areal CFC in the human cortex is observed during VWM and visual attention as well as during resting state. In order to further improve our understanding of CFC, future studies should investigate its role during other cognitive functions, the relationship between local and inter-areal CFC and the relationship between CFC in the cortex and in subcortical structures.

An interesting – and highly challenging – future project that would combine these two lines of research, would be to investigate directionality of cross-frequency interactions with Phase TE, to find out where high-frequency oscillatory processes causally influence low-frequency processes and vice versa. This has remained an open question in the research of cross-frequency coupling and answering this question could greatly advance our understanding of the coordination of feedforward and feedback processes in the brain.

6. Conclusion

In order to understand how cognition is achieved in the human brain, we need to understand how different, functionally specialized regions communicate with each other. Research from over two decades supports the hypothesis that phase synchronization between distinct oscillating neuronal populations is a mechanism that facilitates communication among them and enables complex cognitive function.

However, the analysis of within-frequency phase synchronization does not inform us about the direction of information flow, nor about how integration is achieved between processes in different frequency bands. In study **I**, we introduced a new, phase-based metric of directed connectivity, Phase Transfer Entropy and showed using simulated data that Phase TE can be used to study direction of information flow.

In studies **II-IV**, we investigated inter-areal cross-frequency coupling during visual working memory and visual attention tasks as well as during resting state using data from electrophysiological neuroimaging, and showed that inter-areal cross-frequency phase synchrony and phase-amplitude coupling characterize these different states, connect networks of within-frequency phase synchrony and are functionally relevant. Cross-frequency coupling may hence be crucial for cognitive function by enabling integration of neuronal computations distributed across cortical regions and frequency bands.

Acknowledgements

This thesis work was carried out at the Neuroscience Center, Helsinki Insitute of Life Sciences, and my PhD studies were carried out in the doctoral programme Brain & Mind at the University of Helsinki. In the years 2013-16, I was provided financial support by the doctoral programme.

MEG data acquisition was carried out by my colleagues from the Palva groups and myself at BioMag Laboratory, Helsinki University Central Hospital, and SEEG data was kindly provided by Lino Nobili who recorded it at Claudio Munari Epilepsy Surgery Centre, Niguarda Hospital, Milan, Italy.

I would like to thank my supervisors Satu Palva and Matias Palva for giving me the opportunity to pursue my PhD in their work group and for supporting and encouraging me during these long years. Both have inspired me through their dedication and commitment to scientific research.

Many thanks also go to Professor Juha Voipio for serving as my Custos, to Professor Michael X Cohen for serving as my opponent, and to the pre-examiners of this thesis, Professors Niko Busch and Paul Sauseng, as well as to the members of my thesis committee, Docent Henri Huttunen and Teemu Rinne.

Further thanks go to current and former colleagues, particularly to my frequent collaborators Sheng Wang, characterized by his inspirational work ethic and philosophy; Muriel Lobier, with her admirable dedication to statistics and sarcasm; Santeri Rouhinen, especially for his patient readiness to help with code issues; Hamed Haque, for his cheerful enthusiasm; and further to Tuomas Puoliväli, Gabriele Arnulfo, Jaana Simola, Jonni Hirvonen, Salla Markkinen, Anna Lampinen, Nitin Williams, Isabel Morales-Munoz, Alexander Zhigalov, Sami Karadzeniz and all the others for good collaboration and cameradie.

Further, I would like to thank the coordinator of the Brain & Mind program, Katri Wegelius for her help and advice on organizational matters; and my fellow members of the program's student council in 2015, Zuzanna Miesiewicz, Anna Maria Alexandrou, Sonya Volynets, Onerva Korhonen and Swaroop Achuta for great teamwork in organizing the students' symposium.

I would also like to thank the various teachers and supervisors that throughout my life have guided me, supported and nurtured my interest in science, knowledge and understanding, in particular Ludwig Fischer, Rudolf Wagner, Rudolf Kiefer, Andreas Zilges, Joachim Enders, Deniz Savran, Norbert Pietralla, Michael Wibral, and Danielle Bassett, as well as other figures that have stimulated and influenced my intellectual development, in particular the late Robert Anton Wilson and Willard Boyle.

Many thanks go to my family, my parents Peter and Monika Siebenhühner and my brother Jan Rathje, for all the love and support they have provided me with throughout my life and career, and for all the many different ways in which they have inspired and guided me.

Finally, a million thanks go to my fiancée, Johanna Wahlbeck, who for many years has been a wonderful, supportive, inspiring and loving partner.

Reference List

Akiyama, M., Tero, A., Kawasaki, M., Nishiura, Y., and Yamaguchi, Y. (2017). Theta-alpha EEG phase distributions in the frontal area for dissociation of visual and auditory working memory. *Sci. Rep.* 7, 42776.

Alnaes, D., Sneve, M.H., Richard, G., Skatun, K.C., Kaufmann, T., Nordvik, J.E., Andreassen, O.A., Endestad, T., Laeng, B., and Westlye, L.T. (2015). Functional connectivity indicates differential roles for the intraparietal sulcus and the superior parietal lobule in multiple object tracking. *Neuroimage* 123, 129-137.

Arnulfo, G., Hirvonen, J., Nobili, L., Palva, S., and Palva, J.M. (2015). Phase and amplitude correlations in resting-state activity in human stereotactical EEG recordings. *Neuroimage* 112, 114-127.

Aru, J., Aru, J., Priesemann, V., Wibral, M., Lana, L., Pipa, G., Singer, W., and Vicente, R. (2015). Untangling cross-frequency coupling in neuroscience. *Curr. Opin. Neurobiol.* 31, 51-61.

Axmacher, N., Henseler, M.M., Jensen, O., Weinreich, I., Elger, C.E., and Fell, J. (2010). Cross-frequency coupling supports multi-item working memory in the human hippocampus. *Proc. Natl. Acad. Sci. U. S. A.* 107, 3228-3233.

Axmacher, N., Mormann, F., Fernández, G., Elger, C.E., and Fell, J. (2006). Memory formation by neuronal synchronization. *Brain Research Reviews 52,* 170-182.

Azouz, R., and Gray, C.M. (2003). Adaptive coincidence detection and dynamic gain control in visual cortical neurons in vivo. *Neuron* 37, 513-523.

Bahramisharif, A., Jensen, O., Jacobs, J., and Lisman, J. (2018). Serial representation of items during working memory maintenance at letter-selective cortical sites. *PLoS Biol.* 16, e2003805.

Bastos, A.M., Vezoli, J., Bosman, C.A., Schoffelen, J.M., Oostenveld, R., Dowdall, J.R., De Weerd, P., Kennedy, H., and Fries, P. (2015). Visual Areas Exert Feedforward and Feedback Influences through Distinct Frequency Channels. *Neuron* 85, 390-401.

Belluscio, M.A., Mizuseki, K., Schmidt, R., Kempter, R., and Buzsaki, G. (2012). Cross-frequency phase-phase coupling between theta and gamma oscillations in the hippocampus. *J. Neurosci.* 32, 423-435.

Berger, H. (1929). Uber das Elektroenkephalogramm des Menschen. *Arch. Psychiatr Nervenkr.* 87, 527-570.

Berman, J.I., Liu, S., Bloy, L., Blaskey, L., Roberts, T.P.L., and Edgar, J.C. (2015). Alpha-to-Gamma Phase-Amplitude Coupling Methods and Application to Autism Spectrum Disorder. *Brain Connectivity* 5, 80-90.

Besle, J., Schevon, C.A., Mehta, A.D., Lakatos, P., Goodman, R.R., McKhann, G.M., Emerson, R.G., and Schroeder, C.E. (2011). Tuning of the human neocortex to the temporal dynamics of attended events. *J. Neurosci.* 31, 3176-3185.

Bettencourt, K.C., Michalka, S.W., and Somers, D.C. (2011). Shared filtering processes link attentional and visual short-term memory capacity limits. *J. Vis.* 11, 10.1167/11.10.22.

Bohbot, V.D., Copara, M.S., Gotman, J., and Ekstrom, A.D. (2016). Low-frequency theta oscillations in the human hippocampus during real-world and virtual navigation. *Nature Communications* 8, 14415.

Brookes, M.J., Woolrich, M.W., and Barnes, G.R. (2012). Measuring functional connectivity in MEG: a multivariate approach insensitive to linear source leakage. *Neuroimage* 63, 910-920.

Bruns, A., Eckhorn, R., Jokeit, H., and Ebner, A. (2000). Amplitude envelope correlation detects coupling among incoherent brain signals. *Neuroreport* 5;11(7), 1509-14.

Bruns, A., and Eckhorn, R. (2004). Task-related coupling from high- to low-frequency signals among visual cortical areas in human subdural recordings. *Int. J. Psychophysiol.* 51, 97-116.

Bullmore, E., and Sporns, O. (2009). Complex brain networks: graph theoretical analysis of structural and functional systems. *Nat. Rev. Neurosci.* 10, 186-198.

Busch, N.A., Herrmann, C.S., Muller, M.M., Lenz, D., and Gruber, T. (2006). A cross-laboratory study of event-related gamma activity in a standard object recognition paradigm. *Neuroimage* 33, 1169-1177.

Busch, N.A., and VanRullen, R. (2010). Spontaneous EEG oscillations reveal periodic sampling of visual attention. *Proc. Natl. Acad. Sci. U. S. A.* 107, 16048-16053.

Buschman, T.J., and Miller, E.K. (2007). Top-down versus bottom-up control of attention in the prefrontal and posterior parietal cortices. *Science* 315, 1860-1862.

Bush, D., Bisby, J.A., Bird, C.M., Gollwitzer, S., Rodionov, R., Diehl, B., McEvoy, A.W., Walker, M.C., and Burgess, N. (2017). Human hippocampal theta power indicates movement onset and distance travelled. *Proc. Natl. Acad. Sci. USA* 114, 12297.

Canolty, R.T., Edwards, E., Dalal, S.S., Soltani, M., Nagarajan, S.S., Kirsch, H.E., Berger, M.S., Barbaro, N.M., and Knight, R.T. (2006). High gamma power is phase-locked to theta oscillations in human neocortex. *Science* 313, 1626-1628.

Canolty, R.T., and Knight, R.T. (2010). The functional role of cross-frequency coupling. *Trends Cogn. Sci.* 14, 506-515.

Cardinale, F., Cossu, M., Castana, L., Casaceli, G., Schiariti, M.P., Miserocchi, A., Fuschillo, D., Moscato, A., Caborni, C., Arnulfo, G., and Lo Russo, G. (2013). Stereoelectroencephalography: surgical methodology, safety, and stereotactic application accuracy in 500 procedures. *Neurosurgery* 72, 353-66; discussion 366.

Cavanagh, J.F., and Frank, M.J. (2014). Frontal theta as a mechanism for cognitive control. *Trends Cogn. Sci. (Regul. Ed.)* 18, 414-421.

Chaieb, L., Leszczynski, M., Axmacher, N., Hohne, M., Elger, C.E., and Fell, J. (2015). Theta-gamma phase-phase coupling during working memory maintenance in the human hippocampus. *Cogn. Neurosci.* 1-9.

Cohen, D. (1968). Magnetoencephalography: Evidence of Magnetic Fields Produced by Alpha-Rhythm Currents. *Science* 161, 784.

Cohen, M.X., Axmacher, N., Lenartz, D., Elger, C.E., Sturm, V. and Schlaepfer, T.E. (2009a). Good vibrations: cross-frequency coupling in the human nucleus accumbens during reward processing. *J. Neurosci* 21(5): 875-89

Cohen, M.X., Elger, C.E. and Fell, J. (2009b) Oscillatory activity and phase-amplitude coupling in the human medial frontal cortex during decision making. *J Cogn Neurosci*. 21: 390-402

Cohen, M.X. and Donner, T.H. (2013) Midfrontal conflict-related theta-band power reflects neural oscillations that predict behavior. *J. Neurophysiol.* 110(12): 2752-2763

Colclough, G.L., Woolrich, M.W., Tewarie, P.K., Brookes, M.J., Quinn, A.J., and Smith, S.M. (2016). How reliable are MEG resting-state connectivity metrics? *Neuroimage* 138, 284-293.

Cole, S.R., and Voytek, B. (2017). Brain Oscillations and the Importance of Waveform Shape. *Trends Cogn. Sci.* 21, 137-149.

Corbetta, M., Patel, G., and Shulman, G.L. (2008). The reorienting system of the human brain: from environment to theory of mind. *Neuron* 58, 306-324.

Corbetta, M., and Shulman, G.L. (2002). Control of goal-directed and stimulus-driven attention in the brain. *Nat. Rev. Neurosci.* 3, 201-215.

Culham, J.C., Brandt, S.A., Cavanagh, P., Kanwisher, N.G., Dale, A.M., and Tootell, R.B. (1998). Cortical fMRI activation produced by attentive tracking of moving targets. *J. Neurophysiol.* 80, 2657-2670.

Dale, A.M., Fischl, B., and Sereno, M.I. (1999). Cortical surface-based analysis. I. Segmentation and surface reconstruction. *Neuroimage* 9, 179-194.

David, O., Cosmelli, D., and Friston, K.J. (2004). Evaluation of different measures of functional connectivity using a neural mass model. *Neuroimage* 21, 659-673.

David, O., Cosmelli, D., Hasboun, D., and Garnero, L. (2003). A multitrial analysis for revealing significant corticocortical networks in magnetoencephalography and electroencephalography. *Neuroimage* 20, 186-201.

de Lange, F.P., Jensen, O., Bauer, M., and Toni, I. (2008). Interactions between posterior gamma and frontal alpha/beta oscillations during imagined actions. *Front. Hum. Neurosci.* 2, 7.

de Pasquale, F., Della Penna, S., Snyder, A.Z., Lewis, C., Mantini, D., Marzetti, L., Belardinelli, P., Ciancetta, L., Pizzella, V., Romani, G.L., and Corbetta, M. (2010). Temporal dynamics of spontaneous MEG activity in brain networks. *Proc. Natl. Acad. Sci. U. S. A.* 107, 6040-6045.

Destrieux, C., Fischl, B., Dale, A., and Halgren, E. (2010). Automatic parcellation of human cortical gyri and sulci using standard anatomical nomenclature. *Neuroimage* 53, 1-15.

Doesburg, S.M., Bedo, N., and Ward, L.M. (2016). Top-down alpha oscillatory network interactions during visuospatial attention orienting. *Neuroimage* 132, 512-519.

Doesburg, S.M., Green, J.J., McDonald, J.J., and Ward, L.M. (2009). From local inhibition to long-range integration: a functional dissociation of alpha-band synchronization across cortical scales in visuospatial attention. *Brain Res.* 1303, 97-110.

Drewes, J., and Vanrullen, R. (2011). This is the rhythm of your eyes: the phase of ongoing electroencephalogram oscillations modulates saccadic reaction time. *J. Neurosci.* 31, 4698-4708.

Dugue, L., Marque, P., and VanRullen, R. (2011). The phase of ongoing oscillations mediates the causal relation between brain excitation and visual perception. *J. Neurosci.* 31, 11889-11893.

Emrich, S.M., Riggall, A.C., Larocque, J.J., and Postle, B.R. (2013). Distributed patterns of activity in sensory cortex reflect the precision of multiple items maintained in visual short-term memory. *J. Neurosci.* 33, 6516-6523.

Engel, A.K., and Fries, P. (2010). Beta-band oscillations--signalling the status quo? *Curr. Opin. Neurobiol.* 20, 156-165.

Engel, A.K., Fries, P., and Singer, W. (2001). Dynamic predictions: oscillations and synchrony in top-down processing. *Nat. Rev. Neurosci.* 2, 704-716.

Engel, A.K., and Singer, W. (2001). Temporal binding and the neural correlates of sensory awareness. *Trends Cogn. Sci.* 5, 16-25.

Fell, J., and Axmacher, N. (2011). The role of phase synchronization in memory processes. *Nat. Rev. Neurosci.* 12, 105-118.

Fiebelkorn, I.C., Saalmann, Y.B., and Kastner, S. (2013). Rhythmic sampling within and between objects despite sustained attention at a cued location. *Curr. Biol.* 23, 2553-2558.

Fischl, B. (2012). FreeSurfer. *Neuroimage* 62, 774-781.

Fischl, B., Salat, D.H., Busa, E., Albert, M., Dieterich, M., Haselgrove, C., van der Kouwe, A., Killiany, R., Kennedy, D., Klaveness, S.*, et al.* (2002). Whole brain segmentation: automated labeling of neuroanatomical structures in the human brain. *Neuron* 33, 341-355.

Florin, E., and Baillet, S. (2015). The brain's resting-state activity is shaped by synchronized cross-frequency coupling of neural oscillations. *Neuroimage* 111, 26-35.

Fox, M.D., Corbetta, M., Snyder, A.Z., Vincent, J.L., and Raichle, M.E. (2006). Spontaneous neuronal activity distinguishes human dorsal and ventral attention systems. *Proc. Natl. Acad. Sci. U. S. A.* 103, 10046-10051.

Fox, M.D., Snyder, A.Z., Vincent, J.L., Corbetta, M., Van Essen, D.C., and Raichle, M.E. (2005). The human brain is intrinsically organized into dynamic, anticorrelated functional networks. *Proc. Natl. Acad. Sci. U. S. A.* 102, 9673-9678.

Freunberger, R., Fellinger, R., Sauseng, P., Gruber, W., and Klimesch, W. (2009). Dissociation between phase-locked and nonphase-locked alpha oscillations in a working memory task. *Hum. Brain Mapp.* 30, 3417-3425.

Fries, P. (2015). Rhythms for Cognition: Communication through Coherence. *Neuron* 88, 220-235.

Fries, P. (2005). A mechanism for cognitive dynamics: neuronal communication through neuronal coherence. *Trends Cogn. Sci.* 9, 474-480.

Fries, P., Nikolic, D., and Singer, W. (2007). The gamma cycle. *Trends Neurosci.* 30, 309-316.

Gerber, E.M., Sadeh, B., Ward, A., Knight, R.T., and Deouell, L.Y. (2016). Non-Sinusoidal Activity Can Produce Cross-Frequency Coupling in Cortical Signals in the Absence of Functional Interaction between Neural Sources. *PLoS One* 11, e0167351.

Glennon, M., Keane, M.A., Elliott, M.A., and Sauseng, P. (2016). Distributed Cortical Phase Synchronization in the EEG Reveals Parallel Attention and Working Memory Processes Involved in the Attentional Blink. *Cereb. Cortex* 26, 2035-2045.

Granger, C.W.J. (1969). Investigating Causal Relations by Econometric Models and Cross-spectral Methods. *Econometrica* 37, 424-438.

Gray, C.M., Konig, P., Engel, A.K., and Singer, W. (1989). Oscillatory Responses in Cat Visual-Cortex Exhibit Inter-Columnar Synchronization which Reflects Global Stimulus Properties. *Nature* 338, 334-337.

Griesmayr, B., Berger, B., Stelzig-Schoeler, R., Aichhorn, W., Bergmann, J., and Sauseng, P. (2014). EEG theta phase coupling during executive control of visual working memory investigated in individuals with schizophrenia and in healthy controls. *Cognitive, Affective, & Behavioral Neuroscience* 14, 1340-1355.

Groppe, D.M., Bickel, S., Keller, C.J., Jain, S.K., Hwang, S.T., Harden, C., and Mehta, A.D. (2013). Dominant frequencies of resting human brain activity as measured by the electrocorticogram. *NeuroImage 79,* 223-233.

Haegens, S., Vergara, J., Rossi-Pool, R., Lemus, L., and Romo, R. (2017). Beta oscillations reflect supramodal information during perceptual judgment. *Proc. Natl. Acad. Sci. U. S. A.* 114, 13810-13815.

Hamalainen, M.S., and Ilmoniemi, R.J. (1994). Interpreting magnetic fields of the brain: minimum norm estimates. *Med. Biol. Eng. Comput.* 32, 35-42.

Hamalainen, M.S., and Sarvas, J. (1989a). Realistic conductivity geometry model of the human head for interpretation of neuromagnetic data. *IEEE Trans. Biomed. Eng.* 36, 165-171.

Hamalainen, M.S., and Sarvas, J. (1989b). Realistic conductivity geometry model of the human head for interpretation of neuromagnetic data. *Biomedical Engineering, IEEE Transactions on* 36, 165-171.

Händel, B.F., Haarmeier, T., and Jensen, O. (2011). Alpha oscillations correlate with the successful inhibition of unattended stimuli. *J. Cogn. Neurosci.* 23, 2494-2502.

Hanslmayr, S., Volberg, G., Wimber, M., Dalal, S.S., and Greenlee, M.W. (2013). Prestimulus oscillatory phase at 7 Hz gates cortical information flow and visual perception. *Curr. Biol.* 23, 2273-2278.

Harding, I.H., Yucel, M., Harrison, B.J., Pantelis, C., and Breakspear, M. (2015). Effective connectivity within the frontoparietal control network differentiates cognitive control and working memory. *Neuroimage* 106, 144-153.

Helfrich, R.F., Huang, M., Wilson, G., and Knight, R.T. (2017). Prefrontal cortex modulates posterior alpha oscillations during top-down guided visual perception. *Proc. Natl. Acad. Sci. U. S. A.* 114, 9457-9462.

Herrmann, B., Henry, M.J., Haegens, S., and Obleser, J. (2016). Temporal expectations and neural amplitude fluctuations in auditory cortex interactively influence perception. *Neuroimage* 124, 487-497.

Herrmann, C.S., Munk, M.H., and Engel, A.K. (2004). Cognitive functions of gamma-band activity: memory match and utilization. *Trends Cogn. Sci.* 8, 347-355.

Hipp, J.F., Hawellek, D.J., Corbetta, M., Siegel, M., and Engel, A.K. (2012). Large-scale cortical correlation structure of spontaneous oscillatory activity. *Nat. Neurosci.* 15, 884-890.

Honkanen, R., Rouhinen, S., Wang, S.H., Palva, J.M., and Palva, S. (2015). Gamma Oscillations Underlie the Maintenance of Feature-Specific Information and the Contents of Visual Working Memory. *Cereb. Cortex* 25, 3788-3801.

Howe, P.D., Horowitz, T.S., Morocz, I.A., Wolfe, J., and Livingstone, M.S. (2009). Using fMRI to distinguish components of the multiple object tracking task. *J. Vis.* 9, 10.1-11.

Hummel, F., Andres, F., Altenmüller, E., Dichgans, J., and Gerloff, C. (2002). Inhibitory control of acquired motor programmes in the human brain. *Brain* 125, 404-420.

Hurtado, J.M., Rubchinsky, L.L., and Sigvardt, K.A. (2004). Statistical Method for Detection of Phase-Locking Episodes in Neural Oscillations. *J. Neurophysiol.* 91, 1883-1898.

Hyafil, A., Giraud, A.L., Fontolan, L., and Gutkin, B. (2015). Neural Cross-Frequency Coupling: Connecting Architectures, Mechanisms, and Functions. *Trends Neurosci.* 38, 725-740.

Isler, J.R., Grieve, P.G., Czernochowski, D., Stark, R.I., and Friedman, D. (2008). Cross-frequency phase coupling of brain rhythms during the orienting response. *Brain Res.* 1232, 163-172.

Jensen, O., Bonnefond, M., Marshall, T.R., and Tiesinga, P. (2015). Oscillatory mechanisms of feedforward and feedback visual processing. *Trends Neurosci.* 38, 192-194.

Jensen, O., Kaiser, J., and Lachaux, J.P. (2007). Human gamma-frequency oscillations associated with attention and memory. *Trends Neurosci.* 30, 317-324.

Jensen, O., and Mazaheri, A. (2010). Shaping functional architecture by oscillatory alpha activity: gating by inhibition. *Front. Hum. Neurosci.* 4, 186.

Jensen, O., and Colgin, L.L. (2007). Cross-frequency coupling between neuronal oscillations. *Trends in Cognitive Sciences* 11, 267-269.

Jiang, H., Bahramisharif, A., van Gerven, M.A.J., and Jensen, O. (2015). Measuring directionality between neuronal oscillations of different frequencies. *NeuroImage 118,* 359-367.

Jirsa, V., and Muller, V. (2013). Cross-frequency coupling in real and virtual brain networks. *Front. Comput. Neurosci.* 7, 78.

Jones, K.T., and Berryhill, M.E. (2012). Parietal contributions to visual working memory depend on task difficulty. *Frontiers in psychiatry* 3, 81; 81-81.

Jones, S.R. (2016). When brain rhythms aren't 'rhythmic': implication for their mechanisms and meaning. *Current Opinion in Neurobiology 40,* 72-80.

Jovicich, J., Peters, R.J., Koch, C., Braun, J., Chang, L., and Ernst, T. (2001). Brain areas specific for attentional load in a motion-tracking task. *J. Cogn. Neurosci.* 13, 1048-1058.

Keitel, A., Gross, J., and Kayser, C. (2018). Perceptually relevant speech tracking in auditory and motor cortex reflects distinct linguistic features. *PLoS Biol.* 16, e2004473.

Klimesch, W. (2012). Alpha-band oscillations, attention, and controlled access to stored information. *Trends Cogn. Sci.* 16, 606-617.

Klimesch, W., Sauseng, P., and Hanslmayr, S. (2007). EEG alpha oscillations: the inhibition-timing hypothesis. *Brain Res. Rev.* 53, 63-88.

Konig, P., Engel, A.K., and Singer, W. (1996). Integrator or coincidence detector? The role of the cortical neuron revisited. *Trends Neurosci.* 19, 130-137.

Korhonen, O., Palva, S., and Palva, J.M. (2014). Sparse weightings for collapsing inverse solutions to cortical parcellations optimize M/EEG source reconstruction accuracy. *J. Neurosci. Methods* 226C, 147-160.

Kramer, M.A., Tort, A.B.L., and Kopell, N.J. (2008). Sharp edge artifacts and spurious coupling in EEG frequency comodulation measures. *J. Neurosci. Methods* 170, 352-357.

Kravitz, D.J., Saleem, K.S., Baker, C.I., Ungerleider, L.G., and Mishkin, M. (2013). The ventral visual pathway: an expanded neural framework for the processing of object quality. *Trends Cogn. Sci.* 17, 26-49.

Kulashekhar, S., Pekkola, J., Palva, J.M., and Palva, S. (2016). The role of cortical beta oscillations in time estimation. *Hum. Brain Mapp.* 37, 3262-3281.

Lachaux, J.P., Rodriguez, E., Martinerie, J., and Varela, F.J. (1999). Measuring phase synchrony in brain signals. *Hum. Brain Mapp.* 8, 194-208.

Lakatos, P., Karmos, G., Mehta, A.D., Ulbert, I., and Schroeder, C.E. (2008). Entrainment of neuronal oscillations as a mechanism of attentional selection. *Science* 320, 110-113.

Lakatos, P., Musacchia, G., O'Connel, M.N., Falchier, A.Y., Javitt, D.C., and Schroeder, C.E. (2013). The spectrotemporal filter mechanism of auditory selective attention. *Neuron* 77, 750-761.

Lakatos, P., Shah, A.S., Knuth, K.H., Ulbert, I., Karmos, G., and Schroeder, C.E. (2005). An oscillatory hierarchy controlling neuronal excitability and stimulus processing in the auditory cortex. *J. Neurophysiol. 94(3):1904-11*

Landau, A.N., and Fries, P. (2012). Attention samples stimuli rhythmically. *Curr. Biol.* 22, 1000-1004.

Landau, A.N., Schreyer, H.M., van Pelt, S., and Fries, P. (2015). Distributed Attention Is Implemented through Theta-Rhythmic Gamma Modulation. *Curr. Biol.* 25, 2332-2337.

Lega, B.C., Jacobs, J., and Kahana, M. (2012). Human hippocampal theta oscillations and the formation of episodic memories. *Hippocampus* 22, 748-761.

Lisman, J.E., and Jensen, O. (2013). The theta-gamma neural code. *Neuron* 77, 1002-1016.

Lobier, M., Palva, J.M., and Palva, S. (2017). High-alpha band synchronization across frontal, parietal and visual cortex mediates behavioral and neuronal effects of visuospatial attention. *Neuroimage* 165, 222-237.

López-Muñoz, F., Boya, J., and Alamo, C. (2006). Neuron theory, the cornerstone of neuroscience, on the centenary of the Nobel Prize award to Santiago Ramón y Cajal. *Brain Research Bulletin 70,* 391-405.

Lozano-Soldevilla, D., Ter Huurne, N., and Oostenveld, R. (2016). Neuronal Oscillations with Non-sinusoidal Morphology Produce Spurious Phase-to-Amplitude Coupling and Directionality. *Front. Comput. Neurosci.*

Luck, S.J., and Vogel, E.K. (1997). The capacity of visual working memory for features and conjunctions. *Nature* 390, 279-281.

Maquet, P. (2001). The Role of Sleep in Learning and Memory. *Science* 294, 1048.

Markowitz, D.A., Curtis, C.E., and Pesaran, B. (2015). Multiple component networks support working memory in prefrontal cortex. *Proc. Natl. Acad. Sci. U. S. A.* 112, 11084-11089.

Mathewson, K.E., Gratton, G., Fabiani, M., Beck, D.M., and Ro, T. (2009). To see or not to see: prestimulus alpha phase predicts visual awareness. *J. Neurosci.* 29, 2725-2732.

Michalareas, G., Vezoli, J., van Pelt, S., Schoffelen, J., Kennedy, H., and Fries, P. (2016). Alpha-Beta and Gamma Rhythms Subserve Feedback and Feedforward Influences among Human Visual Cortical Areas. *Neuron 89(2):384-97*

Munk, M.H., Linden, D.E., Muckli, L., Lanfermann, H., Zanella, F.E., Singer, W., and Goebel, R. (2002). Distributed cortical systems in visual short-term memory revealed by event-related functional magnetic resonance imaging. *Cereb. Cortex* 12, 866-876.

Murakami, S., and Okada, Y. (2006). Contributions of principal neocortical neurons to magnetoencephalography and electroencephalography signals. *J. Physiol.* 575, 925-936.

Murty, D.V.P.S., Shirhatti, V., Ravishankar, P., and Ray, S. (2018). Large visual stimuli induce two distinct gamma oscillations in primate visual cortex. *J. Neurosci.*

Nalatore, H., Ding, M., and Rangarajan, G. (2007). Mitigating the effects of measurement noise on Granger causality. *Phys Rev E.* 75, 031123.

Narizzano, M., Arnulfo, G., Ricci, S., Toselli, B., Tisdall, M., Canessa, A., Fato, M.M., and Cardinale, F. (2017). SEEG assistant: a 3DSlicer extension to support epilepsy surgery. - *BMC Bioinformatics* 124.

Nikulin, V.V., and Brismar, T. (2006). Phase synchronization between alpha and beta oscillations in the human electroencephalogram. *Neuroscience* 137, 647-657.

Nikulin, V.V., Linkenkaer-Hansen, K., Nolte, G., Lemm, S., Muller, K.R., Ilmoniemi, R.J., and Curio, G. (2007). A novel mechanism for evoked responses in the human brain. *Eur. J. Neurosci.* 25, 3146-3154.

Nolte, G., Bai, O., Wheaton, L., Mari, Z., Vorbach, S., and Hallett, M. (2004). Identifying true brain interaction from EEG data using the imaginary part of coherency. *Clin. Neurophysiol.* 115, 2292-2307.

Nolte, G., Ziehe, A., Kramer, N., Popescu, F., and Muller, K. (2010). Comparison of Granger Causality and Phase Slope Index.267-276.

Nunez, P.L., Srinivasan, R., Westdorp, A.F., Wijesinghe, R.S., Tucker, D.M., Silberstein, R.B., and Cadusch, P.J. (1997). EEG coherency. I: Statistics, reference electrode, volume conduction, Laplacians, cortical imaging, and interpretation at multiple scales. *Electroencephalogr. Clin. Neurophysiol.* 103, 499-515.

O'Keefe, J., and Recce, M.L. (1993). Phase relationship between hippocampal place units and the EEG theta rhythm. *Hippocampus* 3, 317-330.

Oksama, L., and Hyona, J. (2004). Is multiple object tracking carried out automatically by an early vision
mechanism independent of higher-order cognition? An individual difference approach. *Visual Cognition* 11, 631-671.

O'Neill, G.C., Barratt, E.L., Hunt, B.A., Tewarie, P.K., and Brookes, M.J. (2015). Measuring electrophysiological connectivity by power envelope correlation: a technical review on MEG methods. *Phys Med Biol.* 60(21), 271-95.

Oostenveld, R., Fries, P., Maris, E., and Schoffelen, J.M. (2011). FieldTrip: Open source software for advanced analysis of MEG, EEG, and invasive electrophysiological data. *Comput. Intell. Neurosci.* 2011, 156869.

Palva, J.M., and Palva, S. (2017). Functional integration across oscillation frequencies by cross-frequency phase synchronization. *Eur. J. Neurosci.* 0

Palva, J.M., Monto, S., Kulashekhar, S., and Palva, S. (2010). Neuronal synchrony reveals working memory networks and predicts individual memory capacity. *Proc. Natl. Acad. Sci. U. S. A.* 107, 7580-7585.

Palva, J.M., Palva, S., and Kaila, K. (2005). Phase synchrony among neuronal oscillations in the human cortex. *J. Neurosci.* 25, 3962-3972.

Palva, J.M., Wang, S.H., Palva, S., Zhigalov, A., Monto, S., Brookes, M.J., Schoffelen, J., and Jerbi, K. (2018). Ghost interactions in MEG/EEG source space: A note of caution on inter-areal coupling measures. *NeuroImage 173,* 632-643.

Palva, S., and Palva, J.M. (2012). Discovering oscillatory interaction networks with M/EEG: challenges and breakthroughs. *Trends Cogn. Sci.* 16, 219-230.

Palva, S., and Palva, J.M. (2011). Functional roles of alpha-band phase synchronization in local and large-scale cortical networks. *Front. Psychol.* 2, 204.

Palva, S., and Palva, J.M. (2007). New vistas for alpha-frequency band oscillations. *Trends Neurosci.* 30, 150-158.

Park, H., Ince, R.A., Schyns, P.G., Thut, G., and Gross, J. (2015). Frontal top-down signals increase coupling of auditory low-frequency oscillations to continuous speech in human listeners. *Curr. Biol.* 25, 1649-1653.

Park, H., Lee, D.S., Kang, E., Kang, H., Hahm, J., Kim, J.S., Chung, C.K., and Jensen, O. (2014). Blocking of irrelevant memories by posterior alpha activity boosts memory encoding. *Hum. Brain Mapp.* 35, 3972-3987.

Park, H., Lee, D.S., Kang, E., Kang, H., Hahm, J., Kim, J.S., Chung, C.K., Jiang, H., Gross, J., and Jensen, O. (2016). Formation of visual memories controlled by gamma power phase-locked to alpha oscillations. *Sci. Rep.* 6, 28092.

Pesaran, B., Vinck, M., Einevoll, G.T., Sirota, A., Fries, P., Siegel, M., Truccolo, W., Schroeder, C.E., and Srinivasan, R. (2018). Investigating large-scale brain dynamics using field potential recordings: analysis and interpretation. *Nat. Neurosci.* 21, 903-919.

Petersen, S. ., and Sporns, O. (2015). Brain Networks and Cognitive Architectures. *Neuron* 88, 207-219.

Pylyshyn, Z.W., and Storm, R.W. (1988). Tracking multiple independent targets: evidence for a parallel tracking mechanism. *Spat. Vis.* 3, 179-197.

Raichle, M.E., MacLeod, A.M., Snyder, A.Z., Powers, W.J., Gusnard, D.A., and Shulman, G.L. (2001). A default mode of brain function. *Proc. Natl. Acad. Sci. U. S. A.* 98, 676-682.

Raichle, M.E. (2015). The Brain's Default Mode Network. *Annu. Rev. Neurosci.* 38, 433-447.

Ray, S., and Maunsell, J.H. (2010). Differences in gamma frequencies across visual cortex restrict their possible use in computation. *Neuron* 67, 885-896.

Riggall, A.C., and Postle, B.R. (2012). The relationship between working memory storage and elevated activity as measured with functional magnetic resonance imaging. *J. Neurosci.* 32, 12990-12998.

Roberts, M.J., Lowet, E., Brunet, N.M., Ter Wal, M., Tiesinga, P., Fries, P., and De Weerd, P. (2013). Robust gamma coherence between macaque V1 and V2 by dynamic frequency matching. *Neuron* 78, 523-536.

Roopun, A.K., Kramer, M.A., Carracedo, L.M., Kaiser, M., Davies, C.H., Traub, R.D., Kopell, N.J., and Whittington, M.A. (2008). Period concatenation underlies interactions between gamma and beta rhythms in neocortex. *Front. Cell. Neurosci.* 2, 1.

Rouhinen, S., Panula, J., Palva, J.M., and Palva, S. (2013). Load dependence of beta and gamma oscillations predicts individual capacity of visual attention. *J. Neurosci.* 33, 19023-19033.

Roux, F., and Uhlhaas, P.J. (2014). Working memory and neural oscillations: alpha-gamma versus theta-gamma codes for distinct WM information? *Trends Cogn. Sci.* 18, 16-25.

Roux, F., Wibral, M., Singer, W., Aru, J., and Uhlhaas, P.J. (2013). The Phase of Thalamic Alpha Activity Modulates Cortical Gamma-Band Activity: Evidence from Resting-State MEG Recordings. *J. Neurosci.* 33, 17827.

Rowe, J.B., Toni, I., Josephs, O., Frackowiak, R.S., and Passingham, R.E. (2000). The prefrontal cortex: response selection or maintenance within working memory? *Science* 288, 1656-1660.

Sadaghiani, S., Scheeringa, R., Lehongre, K., Morillon, B., Giraud, A.L., D'Esposito, M., and Kleinschmidt, A. (2012). Alpha-Band Phase Synchrony is Related to Activity in the Fronto-Parietal Adaptive Control Network. *J. Neurosci.* 32, 14305-14310.

Salazar, R.F., Dotson, N.M., Bressler, S.L., and Gray, C.M. (2012). Content-specific fronto-parietal synchronization during visual working memory. *Science* 338, 1097-1100.

Sauseng, P., Klimesch, W., Doppelmayr, M., Pecherstorfer, T., Freunberger, R., and Hanslmayr, S. (2005). EEG alpha synchronization and functional coupling during top-down processing in a working memory task. *Hum. Brain Mapp.* 26, 148-155.

Sauseng, P., Klimesch, W., Freunberger, R., Pecherstorfer, T., Hanslmayr, S., and Doppelmayr, M. (2006). Relevance of EEG alpha and theta oscillations during task switching. *Exp. Brain Res.* 170, 295-301.

Sauseng, P., Klimesch, W., Gruber, W.R., and Birbaumer, N. (2008). Cross-frequency phase synchronization: a brain mechanism of memory matching and attention. *Neuroimage* 40, 308-317.

Sauseng, P., Klimesch, W., Heise, K.F., Gruber, W.R., Holz, E., Karim, A.A., Glennon, M., Gerloff, C., Birbaumer, N., and Hummel, F.C. (2009). Brain oscillatory substrates of visual short-term memory capacity. *Curr. Biol.* 19, 1846-1852.

Sauseng, P., Klimesch, W., Schabus, M., and Doppelmayr, M. (2005). Fronto-parietal EEG coherence in theta and upper alpha reflect central executive functions of working memory. *Int. J. Psychophysiol.* 57, 97-103.

Sauseng, P., Griesmayr, B., Freunberger, R., and Klimesch, W. (2010). Control mechanisms in working memory: A possible function of EEG theta oscillations. *Neuroscience & Biobehavioral Reviews 34,* 1015-1022.

Schack, B., Klimesch, W., and Sauseng, P. (2005). Phase synchronization between theta and upper alpha oscillations in a working memory task. *Int. J. Psychophysiol.* 57, 105-114.

Scheffer-Teixeira, R., Belchior, H., Caixeta, F., Souza, B.C., Ribeiro, S., and Tort, A.B.L. (2012). Theta Phase Modulates Multiple Layer-Specific Oscillations in the CA1 Region. *Cerebral Cortex* 22, 2404-2414.

Scheffer-Teixeira, R., and Tort, A.B. (2016). On cross-frequency phase-phase coupling between theta and gamma oscillations in the hippocampus. *Elife* 5, 10.7554/eLife.20515.

Scheffer-Teixeira, R., and Tort, A.B.L. (2017). Unveiling Fast Field Oscillations through Comodulation. *eNeuro* 4, 10.1523/ENEURO.0079-17.2017. eCollection 2017 Jul-Aug.

Schreiber, T. (2000). Measuring information transfer. *Phys. Rev. Lett.* 85, 461-464.

Schroeder, C.E., and Lakatos, P. (2009). Low-frequency neuronal oscillations as instruments of sensory selection. *Trends Neurosci.* 32, 9-18.

Schroeder, C.E., Lakatos, P., Kajikawa, Y., Partan, S., and Puce, A. (2008). Neuronal oscillations and visual amplification of speech. *Trends Cogn. Sci.* 12, 106-113.

Schroeder, S.C.Y., Ball, F., and Busch, N.A. (2018). The role of alpha oscillations in distractor inhibition during memory retention. *Eur. J. Neurosci.* 48, 2516-2526.

Senoussi, M., Moreland, J.C., Busch, N.A., and Dugue, L. (2018). Attention explores space periodically at the theta frequency. *bioRxiv* 443341.

Shannon, C.E. (1948). A mathematical theory of communication. *Bell system technical journal* 27,

Siegel, M., Donner, T.H., Oostenveld, R., Fries, P., and Engel, A.K. (2008). Neuronal synchronization along the dorsal visual pathway reflects the focus of spatial attention. *Neuron* 60, 709-719.

Singer, W. (2009). Distributed processing and temporal codes in neuronal networks. *Cogn. Neurodyn* 3, 189-196.

Singer, W. (1999). Neuronal synchrony: a versatile code for the definition of relations? *Neuron* 24, 49-65, 111-25.

Sreenivasan, K.K., Curtis, C.E., and D'Esposito, M. (2014). Revisiting the role of persistent neural activity during working memory. *Trends Cogn. Sci.* 18, 82-89.

Stam, C.J., Nolte, G., and Daffertshofer, A. (2007). Phase lag index: assessment of functional connectivity from multi channel EEG and MEG with diminished bias from common sources. *Hum. Brain Mapp.* 28, 1178-1193.

Tallon-Baudry, C., and Bertrand, O. (1999). Oscillatory gamma activity in humans and its role in object representation. *Trends Cogn. Sci.* 3, 151-162.

Tallon-Baudry, C., Bertrand, O., Delpuech, C., and Pernier, J. (1996). Stimulus specificity of phase-locked and non-phase-locked 40 Hz visual responses in human. *J. Neurosci.* 16, 4240-4249.

Tallon-Baudry, C., Bertrand, O., and Fischer, C. (2001). Oscillatory synchrony between human extrastriate areas during visual short-term memory maintenance. *J. Neurosci.* 21, art. no.-RC177.

Tallon-Baudry, C., Mandon, S., Freiwald, W.A., and Kreiter, A.K. (2004). Oscillatory synchrony in the monkey temporal lobe correlates with performance in a visual short-term memory task. *Cereb. Cortex* 14, 713-720.

Tass, P., Rosenblum, M.G., Weule, J., Kurths, J., Pikovsky, A., Volkmann, J., Schnitzler, A., and Freund, H.J. (1998). Detection of n : m phase locking from noisy data: Application to magnetoencephalography. *Phys. Rev. Lett.* 81, 3291-3294.

Tort, A.B., Komorowski, R., Eichenbaum, H., and Kopell, N. (2010). Measuring phase-amplitude coupling between neuronal oscillations of different frequencies. *J. Neurophysiol.* 104, 1195-1210. d

Tort, A.B., Kramer, M.A., Thorn, C., Gibson, D.J., Kubota, Y., Graybiel, A.M., and Kopell, N.J. (2008). Dynamic cross-frequency couplings of local field potential oscillations in rat striatum and hippocampus during performance of a T-maze task. *Proc. Natl. Acad. Sci. U. S. A.* 105, 20517-20522.

Treisman, A. (2006). How the deployment of attention determines what we see. *Vis. cogn.* 14, 411-443.

Uhlhaas, P.J., Pipa, G., Lima, B., Melloni, L., Neuenschwander, S., Nikolic, D., and Singer, W. (2009). Neural synchrony in cortical networks: history, concept and current status. *Front. Integr. Neurosci.* 3, 17.

van der Meij, R., Kahana, M., and Maris, E. (2012). Phase-amplitude coupling in human electrocorticography is spatially distributed and phase diverse. *J. Neurosci.* 32, 111-123.

van Driel, J., Knapen, T., van Es, D.M. and Cohen, M.X. (2014). Interregional alpha-band synchrony supports temporal cross-modal integration. *NeuroImage* 101*:* 404-415.

van Driel, J., Cox, R., and Cohen, M.X. (2015). Phase-clustering bias in phase–amplitude cross-frequency coupling and its removal. *Journal of Neuroscience Methods* 254*,* 60-72.

Vanderwolf, C.H. (1969). Hippocampal electrical activity and voluntary movement in the rat. *Electroencephalography and Clinical Neurophysiology 26,* 407-418.

Vanhatalo, S., Palva, J.M., Holmes, M.D., Miller, J.W., Voipio, J., and Kaila, K. (2004). Infraslow oscillations modulate excitability and interictal epileptic activity in the human cortex during sleep. *Proc. Natl. Acad. Sci. U. S. A.* 101, 5053-5057.

Vertes, R.P. (1977). Selective firing of rat pontine gigantocellular neurons during movement and REM sleep. *Brain Research* 128*,* 146-152.

Vidal, J.R., Chaumon, M., O'Regan, J.K., and Tallon-Baudry, C. (2006). Visual grouping and the focusing of attention induce gamma-band oscillations at different frequencies in human magnetoencephalogram signals. *J. Cogn. Neurosci.* 18, 1850-1862.

Vinck, M., Oostenveld, R., van Wingerden, M., Battaglia, F., and Pennartz, C.M. (2011). An improved index of phase-synchronization for electrophysiological data in the presence of volume-conduction, noise and sample-size bias. *Neuroimage* 55, 1548-1565.

Voloh, B., Valiante, T.A., Everling, S., and Womelsdorf, T. (2015). Theta-gamma coordination between anterior cingulate and prefrontal cortex indexes correct attention shifts. *Proc. Natl. Acad. Sci. U. S. A.* 112, 8457-8462.

Wang, S., Lobier, L., Siebenhühner, F., Puoliväli, T., Palva, S., and Palva, J. (2018). Hyperedge bundling: A practical solution to spurious interactions in MEG/EEG connectivity analyses. *NeuroImage* 173: 610-622.

Wang, X.J. (2010). Neurophysiological and computational principles of cortical rhythms in cognition. *Physiol. Rev.* 90, 1195-1268.

Watrous, A.J., Deuker, L., Fell, J., and Axmacher, N. (2015). Phase-amplitude coupling supports phase coding in human ECoG. *Elife* 4, 10.7554/eLife.07886.

Wiener, N. (1956). The theory of prediction. In Modern Mathematics for the Engineer, Beckmann, E. F. ed., (New York: McGraw-Hill)

Winson, J. (1974). Patterns of hippocampal theta rhythm in the freely moving rat. *Electroencephalography and Clinical Neurophysiology* 36*,* 291-301.

Xu, X., Zheng, C., and Zhang, T. (2013). Reduction in LFP cross-frequency coupling between theta and gamma rhythms associated with impaired STP and LTP in a rat model of brain ischemia. *Frontiers in Computational Neuroscience* 7, 27.

Zheng, C., and Zhang, T. (2013). Alteration of phase-phase coupling between theta and gamma rhythms in a depression-model of rats. *Cognitive Neurodynamics* 7, 167-172.

Recent Publications in this Series

15/2019 Jana Buzkova
The Metabolic and Molecular Consequences of Mitochondrial Dysfunction in Mitochondrial Disease and Acquired Obesity
16/2019 Ilmar Efendijev
Cardiac Arrest Patients in Finnish Intensive Care Units: Insights into Incidence, Long-Term Outcomes and Costs
17/2019 Emma Komulainen
Early Effects of Antidepressants on Emotional Processing
18/2019 Henna Pehkonen
Liprin-α1 in Cancer Cell Adhesion Machinery and Tumor Progression
19/2019 Velma T. E. Aho
Differential Abundance Analyses of Human Microbiota in Parkinson's Disease
20/2019 Tiina Viita
Analysis of Nuclear Actin-Interacting Proteins and Actin-Regulated Transcription Factors
21/2019 Roland Zimm
On the Development of the Turtle Scute Pattern and the Origins of Its Variation
22/2019 Terhi Lohela
Quality of Care and Access to Care at Birth in Low- and Middle-Income Countries
23/2019 Anna Svärd
Body Weight and Mental Health: A Follow-Up Study on Health Functioning and Work Disability
24/2019 Zuzanna Misiewicz
What Makes Us Anxious: A Cross-Species Multi-omics Approach to the Biological Basis of Anxiety Disorders
25/2019 Saku Torvinen
Health-Related Quality of Life and Costs in Prostate Cancer
26/2019 Anu Haaramo
Oral Manifestations in Crohn´s Disease and Orofacial Granulomatosis
27/2019 Abdelhakim Salem
Histamine H4 Receptor: A Potential Novel Therapeutic Target in Oral Lichen Planus and Oral Tongue Cancer
28/2019 Lauri Puustinen
Autoimmune Hepatitis: Epidemiology, Prognosis and Follow-Up
29/2019 Agnes Stenius-Ayoade
Housing, Health and Service Use of the Homeless in Helsinki, Finland
30/2019 Mari Metsäniitty
Forensic Age Assessment in Finland, and Dental Development of Somalis
31/2019 Heli Tolppanen
Prognostication in Acute Heart Failure and Cardiogenic Shock— Focus on Electrocardiography and Biomarkers
32/2019 Olli-Pekka Pulkka
Novel Therapeutic Targets in Gastrointestinal Stromal Tumor
33/2019 Inkeri Spoljaric
GABAergic Signaling and Neuronal Chloride Regulation in the Control of Network Events in the Immature Hippocampus
34/2019 Nina Mars
Healthcare Utilization in Rheumatic Diseases
35/2019 Katrina Albert
Modelling Alpha-Synuclein-Based Parkinson's Disease and Studies with CDNF

Helsinki 2019 ISSN 2342-3161 ISBN 978-951-51-5219-0